MEASUREMENT OF DIFFUSION COEFFICIENT OF ETHANOL IN PURE WATER BY USING MOIRÉ DEFLECTOMETRY TECHNIQUE

BY: - GUYITA KUSSIA

A Thesis submitted to

The department of applied physics,

School of applied natural sciences,

Presented in partial fulfilment the requirement for the degree of master's in physics

Office of Graduate Studies

Adama Science and Technology University

Adama

August, 2017

MEASUREMENT OF THE DIFFUSION COEFFICIENT OF ETHANOL IN PURE WATER BY USING MOIRÉ DEFLECTOMETRY TECHNIQUE

BY: - GUYITA KUSSIA

ADVISOR: - ALEMU KEBEDE (PhD)

A Thesis Submitted to
The Department of Applied Physics,
School of Applied Natural Sciences,
Presented in Partial Fulfilment of the Requirement for the Degree of Master's in Physics

Office of Graduate Studies
Adama Science and Technology University

Adama
August, 2017

Declaration

I hereby declare that this MSc Thesis dissertation is my original work and has not been presented for a degree in any other university, and all sources of material used for this thesis dissertation have been duly acknowledged.

Name: - Guyita Kussia

Signature: - _____

Date: - _____

This MSc thesis dissertation has been submitted for examination with my approval as thesis advisor /dissertation supervisor.

Name: - ALEMU KEBEDE (PhD)

Signature: - _____

Date: - _____

Adama Science and Technology University Graduate Studies Program

Examination Committee Approval Sheet

This is to certify that the Thesis prepared by **Guyita Kussia: - "Measurement of Diffusion Coefficient of Ethanol in Pure Water by Using Moiré Defelectometry Technique"** and submitted for partial fulfillment of the requirement for the degree of mater of Science in physics Complies with the regulation of the University meets the accepted standards with Respect to Originality and quality**.**

Signed By the Examining Committee

_____	_____
Chairman	signature
_____	_____
Advisor	Signature
_____	_____
Examiner (Internal)	Signature
_____	_____
Examiner (External)	Signature
_____	_____

Dedication

This work is dedicated to my late mother. May her soul rest in peace.

ACKNOWLEDGEMENTS

First and foremost, I thank God for everything was possible in his will. I want to express my deep gratitude to my advisor Dr. Alemu Kebede for his initiation, his continues follow up, motivation, and his smooth but efficient communication throughout the research. I would like to thank Dr. Abebe Belay for providing me diffusion cell (cuvette). And I want to thank Mr. Debebe who welcomed me in the lab warm heartedly and for his technical assistance.

I would like to thank Meselech Bali for the provision of digital camera. I am also grateful to my class mates and staffs, Girum Siyoum, Abdulkadir Abdo, Galgalo Liban and Addisu Iticha. I'm highly indebted to my brothers Mathias kussia and Abenezer Kussia for giving me moral and support throughout the project. My whole hearted acknowledgement goes to Adama Science and Technology University in general and department of physics in particular for their coordinated work.

Finally, I would like to thank MOE for their financial support to do my project.

Table of content

Contents **page**

List of table iii
List of figures iv
List of Abbreviation and Acronyms vi
ABSTRACT vii
CHAPTER ONE 1
Introduction 1
1.2. Statement of the problem 4
1.3.1. Specific objectives 5
1.4. Significance of the study 5
Review of related literature 6
2.1. Ethanol 6
2.2. Diffusion 8
2.2.1. The theoretical basis of diffusion 9
2.2.2. Basic hypothesis of mathematical theory of diffusion 10
2.2.3. Differential equation of diffusion 11
2.2.4. The empirical laws of diffusion 13
2.2.5. Diffusion coefficient and mean free path 15
2.2.6. Diffusion coefficient and viscosity 16
2.2.7. Random walk as a statistical model for diffusion 18
(One-dimensional treatment) 18
2.3. Moiré pattern and moiré defelectometry 20
2.3.1 Interference of fringes on screen 20
2.3.1.1 Theory of interference 20
2.3.2. Diffraction 23
2.3.2.1. The plane diffraction grating 23
2.3.3 Moiré and fringe projection techniques 23
2.3.3.1 What is Moiré pattern? 24
2.3.3.2. Fringe projection techniques 29

2.3.3.3 Shadow Moiré 31
2.3.3.4 Projection Moiré 34
2.3.4. Moiré Defelectrometry 35
2.3.4.1 Phase measuring defelectrometry 38
CHAPTER THREE 45
Experimental Technique 45
3.1. Materials used 45
3.3. Experimental procedures 46
CHAPTER FOUR 48
Results, Analysis and Discussion 48
4.1. Determination of diffusion coefficient of ethanol solution in different concentration 48
4.1.1. Results obtained for 5 % of ethanol solution 48
4.1.2. Results obtained for 10 % of ethanol solution 49
4.1.3. Results obtained for 15 % of ethanol solution 49
4.1.4. Results obtained for 20 % of ethanol solution 50
4.1.5. Results obtained for 25 % for ethanol solution 50
4.1.6. Results obtained for 30% of ethanol solution 51
4.1.7. Results obtained for 35 % of ethanol solution 51
4.1.8. Results obtained for 40 % of ethanol solution 52
4.1.9. Results obtained for 50% of ethanol solution 52
4.2. Discussion 53
4.3. Diffusion Vs concentration graph 54
CHAPTER FIVE 55
Conclusion and Recommendation 55
5.1. Conclusion 55
5.2. Recommendation 55
BIBLIOGRAPHY 56

List of table

Pages

Table 1. Fringe Shifts in 5 percent of Ethanol solution after $t_0 = 0, t_1 = 90\text{min. and } t_2 = 2hr$ ----------48

Table2. Fringe Shifts in 10 percent of Ethanol solution after $t_0 = 0, t_1 = 2\text{hr. and } t_2 = 2\frac{1}{2}\text{hr}$ ---------- 49

Table 3. Fringe Shifts in 15 percent of Ethanol solution after $t_0 = 0, t_1 = 2\frac{1}{2}\text{hr and } t_2 = 3\text{hr}$----------49

Table 4. Fringe Shifts in 20 percent of Ethanol solution after $t_0 = 0, t_1 = 3\text{hr. and } t_2 = 3\frac{1}{2}\text{hr}$----------50

Table.5. Fringe Shifts in 25 percent of ethanol solution after $t_0 = 0, t_1 = 3\frac{1}{2}\text{hr. and } t_2 = 4\text{hr}$----------50

Table 6. Fringe Shifts in 30 percent of Ethanol solution after $t_0 = 0, t_1 = 4\text{hr. and } t_2 = 5\text{hr}$ ----------51

Table 7. Fringe Shifts in 35 percent of Ethanol solution after $t_0 = 0, t_1 = 5\text{hr. and } t_2 = 5\frac{1}{2}\text{hr}$ ----------51

Table 8. Fringe Shifts in 40 percent of Ethanol solution after $t_0 = 0, t_1 = 6\text{hr and } t_2 = 6\frac{1}{2}\text{hr}$ ----------52

Table 9. Fringe Shifts in 50 percent of Ethanol solution after $t_0 = 0, t_1 = 8\text{hr and } t_2 = 9\text{hr}$ ----------52

Table 10. The result of slops and intercept for Diffusion Vs concentration graph----------54

List of figures

Pages

Fig 1. The motions of molecules or atoms appears to be random walk----------10

Fig 2. The rate of transfer of diffusing of atoms per unit area of section----------11

Fig 3. Element of Volume----------12

Fig 4. Diffusion and random motion ----------19

Fig 5. Interference of monochromatic light----------20

Fig 6. Moiré fringes at small angle tilt----------24

Fig 7. Moiré between two straight-line gratings of the same pitch at angle 2α with respect to each other----------25

Fig 8. Moiré pattern caused by two straight-line gratings----------27

Fig 9. Geometry used to determine spacing and angle between two gratings of different frequencies----------28

Fig 10. Projection of fringes or gratings onto an object and observing it at angle α. ----------30

Fig 11. Maximum sensitivity for fringe projection at 90^0 angle between projection and viewing ----------31

Fig12. Fringe produced by two interfering beams----------31

Fig 13. Geometry for shadow moiré where illumination and viewing points are at infinity----------32

Fig 14. Shadow moiré when both illumination and viewing positions are at finite distances----------33

Fig 15. Projection moiré where fringes or a grating are projected onto a surface and viewed through a second grating ----------34

Fig 16. Experimental arrangement of laser Moiré defelectometery----------36

Fig 17. Spatial frequency distribution of moiré fringes----------40

Fig 18. Plastic bottles used to keep different concentration of ethanol and the diffusion cell----------45

Fig 19. Experimental set up viewing from near digital camera and near **He-Ne** laser----------46

Fig 4.1. Fringe Shift in 5% of Ethanol solution----------48

Fig 4.2. Fringe Shift in 10% of Ethanol solution----------49
Fig 4.3. Fringe Shift in 15 % of Ethanol solution----------49
Fig 4.4. Fringe Shift in 20 % of Ethanol solution---------- 50
Fig 4.5. Fringe Shift in 25% of Ethanol solution----------50
Fig 4.6. Fringe Shift in 30% of Ethanol solution----------50
Fig 4.7. Fringe Shift in 35 % of Ethanol solution----------51
Fig 4.8. Fringe Shift in 40% of Ethanol solution----------51
Fig 4.9. Fringe Shift in 50% of Ethanol solution----------52
Fig 4.3.1 Diffusion Vs concentration graph----------54

List of Abbreviation and Acronyms

ESPI----------Electronic Speckle Pattern Interferometry

BE----------Beam Expander

TWH----------Two Wavelength Holography

CCD----------Charge-Coupled Device (Digital Camera)

MOE----------Ministry of education

ABSTRACT

In this research work measurement of diffusion coefficient of two miscible liquids is reported. The liquids are various combinations of ethanol and pure water. Moiré Defelectometry method was used in order to measure the diffusion coefficient of ethanol solution in pure water at room temperature (23$\pm$2 ^0C). The apparatus were: He-Ne laser (λ= 632.8 nm), expanding and collimating lenses, the diffusion cell, two similar rhonchi gratings, thermometer, syringes, screen, CCD camera and computer, and they were carefully calibrated and adequate operating conditions were summarized. Measured with this apparatus, the average diffusion coefficient (D) of Ethanol solution in pure water, agree with those reported value in literature, which is D = (0.822 $\pm$ 0.02) X $10^{-9}m^2/s$ assuming that the diffusion process is one-dimensional. It is found that the diffusion coefficient of ethanol solutions increases linearly with increase in solute concentration.

Key Words: - *Moiré Defelectometery, Fringe Projection, Moiré Fringes, Transmission Grating, Index of Refraction, Moiré fringe shift, Diffusion Coefficient, Concentration*

CHAPTER ONE

Introduction

Alcoholic beverages are class of organic compounds, containing one or more hydroxyl group (OH), attached to a carbon atom. Ethanol (ethyl alcohol, grain alcohol) is a clear, colorless liquid with a characteristic, agreeable odor. Ethanol is the only type of alcohol that can be prepared and consumed at a commercial or household level. Alcoholic beverages can be produced by fermentation and/or distillation and distilled alcoholic spirit categories that include two groups in itself: namely distilled spirits and liquors [1]. Fermented drinks are prepared by the action of yeasts that metabolize sugars or other carbohydrates in grapes, other fruits, vegetables and grains by producing alcohol as a waste product whereas distilled spirits are produced by the distillation of fermented raw materials with the separation of alcohol from fermented liquid by increasing the alcohol content. Wine, Beer, whisky, rum, vodka, brandy, gin and liquor are the most consumed alcoholic beverages all around the world [2, 3].

In many countries there are beverages which either fall outside of the usual beer, wine and spirits categories or which are traditionally produced at the local level, for example in villages and in homes. This kind of production seems especially common in many African countries, where a wide variety of different beverages can be found. Many of these are produced by fermentation of seeds, grains, fruit, and vegetables or from palm trees, which is a rather simple procedure. In Ethiopia, very popular traditional fermented alcoholic drinks include "tella" [4], "tej" [5], "areke" [6], "borde" [7], and "shamita" [8]. The *borde* and *shamita* are mainly prepared in central and southern Ethiopia [9, 10] whereas considering popularity, traditional alcoholic beverages namely, *tella* and 'katikala' (*areke)* is very common in northern part of Ethiopia. Currently, even bottled 'Gojam *areke'* from north Ethiopia is in the market by gathering from different rural vending houses.

"Areke" is a traditional home-distilled beverage that is made from an assortment of cereals such as wheat, sorghum and maize, and has a high level of ethanol. "*Areke"* is usually brewed in rural and semi-urban areas and is used more commonly by farmers and semi-urban dwellers than by people who live in the cities. In cities, those who drink "*areke"* are predominantly lower class people or those who have become dependent on alcohol and cannot afford to buy industrially produced alcohol [11]. Ethanol(pure) crystalizes at –114.1°C, boils at 78.5°C, and has a density of 0.789 g/ml at 20°C. Its low freezing point has made it useful as the fluid in thermometers for temperatures below –40°C, the freezing point of mercury, and for other low-temperature purposes, such as for antifreeze in automobile radiators. Ethanol is miscible in all proportions with water and with most organic solvents. This means it can diffuse easily in water and most organic solvents [12, 13].

Diffusion is a process by which matter is transformed from one part of a system to another as a result of random molecular motion [14, 15]. The diffusion in the stationary liquid or gas phase is characterized by diffusion coefficient. The diffusion coefficient of a substance in a fluid can be predicted theoretically or found from empirical correlations. It can also be obtained experimentally. Optical methods are among the wide variety of techniques available. They apply to transparent fluids and are based on the fact that the concentration distribution in a diffusion process produces a gradient in the index of refraction within the fluid.

Diffusion in transparent liquids can be studied by various optical methods based on the measurement of refractive index variation, such as, for example, interferometry, holographic interferometry, sandwich holography, electronic Speckle pattern interferometry (ESPI), speckle decor relation, scanning laser beam, and common path interferometry [16]. Laser-based techniques are among the most sensitive methods employed for measuring diffusion coefficient and thermal conductivity. But the main limitation of the interferometric methods is their sensitivity to vibrations, and so they require precise optical conditions and limits their implementation in an industrial environment[16].

In this report the we use a high-precision, real-time, noninvasive, laser-based technique to measure the refractive index of a liquid mixture or an aqueous solution, which includes the Moiré defelectometry technique for direct mapping of ray deflection due to change in refractive index of a medium. Moiré defelectometry is a simple technique for optical testing of phase objects and specular surfaces, based on the moiré effect. The method provides mapping of ray deflections caused by either a phase object or reflection from a surface. Moiré defelectometry is a simple and powerful tool for measuring ray deflections within the paraxial approximation.

The main advantages of the Moiré defelectometry technique are its extreme experimental simplicity, low cost and low sensitivity to external disturbances in comparison with other interferometric methods that requires high precision and stable experimental set-up. In a transparent mixture, change in concentration, for a multi-component liquid mixture, and temperature, results a change in the liquid index of refraction. A parallel laser beam, passing through such a medium of varying index of refraction, is locally deflected even if it passes perpendicularly to the gradient of the index of refraction (diffusion direction). The deflection angle is direct mapping of the refractive index gradient of the medium [16].

The Moiré Defelectrometry method is used by other researchers to find the diffusion coefficient of sugar solution, Kazem Jamshidi-Ghaleh and et al [17]. In this report the Moiré defelectometry method was applied for measuring the diffusion coefficient of Ethanol solution in pure water under 5-mW He–Ne laser (λ=632.8 nm) illumination and its value was compared to the reported measurements in the literature which are carried out using other methods such as Cussler, E. L. empirical correlation method [18], Wilke.C.R. Experimental and theoretical correlation method [19].The study was organized in five chapters. The first chapter is the introductory chapter that includes the statement of the problem, the general and specific objectives, and the significance of the study. In Chapter two the definition of ethanol, diffusion and the principle of Moiré defelectometry is given and a review of the publications within this field is presented in detail. In Chapter three the experimental methods (materials used, experimental setup, and

procedure) for this thesis work are presented. Chapter four includes the detail of results, data analysis and discussion. Finally, Chapter five includes conclusions and the outlooks into future work were presented.

1.2. Statement of the problem

The diffusion coefficient of a substance in a fluid can be predicted theoretically or found from empirical correlations. It can also be obtained experimentally. Optical methods are among the wide variety of techniques available, such as, interferometry, holographic interferometry, sandwich holography, electronic Speckle pattern interferometry (ESPI), speckle decor relation, scanning laser beam, and common path interferometry [16]. Laser-based techniques are among the most sensitive methods employed for measuring diffusion coefficient and thermal conductivity.

Moiré defelectometry is one of a simple and powerful tool for measuring ray deflections within the paraxial approximation. This technique is chosen for its extreme experimental simplicity, low cost and low sensitivity to external disturbances in comparison with other interferometric methods that requires high precision and stable experimental set-up. The method was used by other researchers to find the diffusion coefficient of sugar solution, Kazem Jamshidi-Ghaleh and et al. [17].As far as my knowledge is concerned, no investigation has been done on Ethanol using Moiré defelectometry. Therefore, based on the above investigation the study aims to use Moiré defelectometry method for measuring the diffusion coefficient of Ethanol solution in pure water under 5-mW He–Ne laser (λ=632.8 nm) illumination and its value was compared to the reported measurements in the literature which are carried out using other methods such as Cussler, E. L. empirical correlation method [18], Wilke.C.R. Experimental theoretical correlation method [19].

1.3. General objective

The general objective of this study is to determine the diffusion coefficient of ethanol solution in pure water using moiré defelectometery technique.

1.3.1. Specific objectives

The Specific objectives of this study are:

i. to determine the diffusion coefficient of different concentration of Ethanol in pure water using Moiré defelectometry technique.

ii. to compare the diffusion coefficient of different concentration of Ethanol in pure water.

1.4. Significance of the study

As mentioned above the general objective of the study is to determine the diffusion coefficient of ethanol solution in pure water using moiré defelectometery technique. And this study expected to be helpful for the following:-

- It helps to approve the quality of Ethanol for the daily users.
- It helps the factory to maximize the quality of its product and have more customers.
- It helps the factory to be competitive in the world market and this may reduce the foreign currency with those kinds of ethanol were imported to our country.

Finally, this study may also help those who like to study similar research as a reference.

CHAPTER TWO

Review of related literature

2.1. Ethanol

Ethanol (ethyl alcohol, grain alcohol) is a clear, colorless liquid with a characteristic, agreeable odor. In dilute aqueous solution, it has a somewhat sweet flavor, but in more concentrated solutions it has a burning taste. Ethanol, CH_3CH_2OH, is an alcohol, a group of chemical compounds whose molecules contain a hydroxyl group,–OH, bonded to a carbon atom. The word alcohol derives from Arabic al-kuhul, which denotes a fine powder of antimony used as an eye makeup. Alcohol originally referred to any fine powder, but medieval alchemists later applied the term to the refined products of distillation, and this led to the current usage. Ethanol crystalizes at –114.1°C, boils at 78.5°C, and has a density of 0.789 g/mL at 20°C. Its low freezing point has made it useful as the fluid in thermometers for temperatures below –40°C, the freezing point of mercury, and for other low-temperature purposes, such as for antifreeze in automobile radiators [12,13].

It is made from the fermentation or chemical breakdown of sugars by yeasts. All beverage ethanol and more than half of industrial ethanol is still made by this process. And also it is made from plants and grains such as corn, wheat, barley. In the production of beverages, such as whiskey and brandy, the impurities supply the flavor. Starches from potatoes, corn, wheat, and other plants can also be used in the production of ethanol by fermentation. During the fermentation process, the starches of the grains are turned into alcohol. The fermentation reaction is represented by this simple equation:

$$C_6H_{12}O_6 \longrightarrow 2\ CH_3CH_2OH + 2\ CO_2 \qquad (1)$$

The ethanol produced by fermentation ranges in concentration from a few percent up to about 14 percent. Above about 14 percent, ethanol destroys the zymase enzyme and fermentation stops. Ethanol is normally concentrated by distillation of aqueous solutions,

but the composition of the vapor from aqueous ethanol is 96 percent ethanol and 4 percent water. Therefore, pure ethanol cannot be obtained by distillation. Commercial ethanol contains 95 percent by volume of ethanol and 5 percent of water. Dehydrating agents can be used to remove the remaining water and produce absolute ethanol [11].Ethanol Alcohol is commonly used in the medical field as an antiseptic and as a disinfectant. Medical wipes and antibacterial hand sanitizers have alcohol to help prevent the spreading of bacteria in hospitals and related facilities. Alcohol is also used to sterilize the skin before injections. Hospitals and medical clinics use alcohol to sterilize various medical equipment before and after use [11, 12].

Ethanol is also used as an automotive fuel by itself and can be mixed with gasoline to form gasohol. The gasohol Contains 15% of ethanol and 85% of gasoline. The majority of all our energy needs come from fossil fuels. The gasoline (fossil fuel) reserves are finite and being used at accelerating rate, and faces depletion. We need alternative energy sources. To reduce consumption of nonrenewable fossil fuels and to sustain our way of life ethanol is seem to be a suitable renewable source of energy. It can be used as a petrol extender and therefore reduce the consumption of petrol. It undergoes a complete combustion leading to cleaner exhaust gases (emits less CO and CO_2) [12, 13].

It can be safely used as a solvent for different products such as perfumes, paints, lacquer, and explosives, culinary extracts, essential oils, tinctures, and concentrates. Using Food Grade Ethyl Alcohol will minimize the impurities that can contaminate your extracts and tinctures. It also leaves little to no residual. Ethyl Alcohol is often used as a final wash when making BHO and CO_2 extractions. Most industrial ethanol is denatured to prevent its use as a beverage. Denatured ethanol contains small amounts, 1 or 2 percent each, of several different unpleasant or poisonous substances. Ethanol is toxic, and the body begins to dispose of it immediately upon its consumption. Over 90 percent of it is processed by the liver. In the liver, the alcohol dehydrogenase enzyme converts ethanol into acetaldehyde, which is itself toxic [11, 13].

Ethanol acts as a drug affecting the central nervous system. Its behavioral effects stem from its effects on the brain and not on the muscles or senses themselves. It is a depressant, and depending on dose, can be a mild tranquilizer or a general anesthetic. It suppresses certain brain functions. At very low doses, it can appear to be a stimulant by suppressing certain inhibitory brain functions. However, as concentration increases, further suppression of brain functions produce the classic symptoms of intoxication: slurred speech, unsteady walk, disturbed sensory perceptions, and inability to react quickly. At very high concentrations, ethanol produces general anesthesia; a highly intoxicated person will be asleep and very di Alcohol levels in the brain are difficult to measure, and so blood alcohol levels are used to assess degree of intoxication [11, 12, and 13].

Most people begin to show measurable mental impairment at around 0.05 percent blood alcohol. At around 0.10 percent, mental impairment will show obvious physical signs, such as an unsteady walk. Slurred speech shows up at around 0.15 percent. Unconsciousness results by 0.4 percent. Above 0.5 percent, the breathing center of the brain or the beating action of the heart can be anesthetized, resulting in death. Difficult to wake, and if awakened, unable to move voluntarily. Ethanol is miscible in all proportions with water and with most organic solvents. This means ethanol can diffuse easily in water and most organic solvents [11, 12].

2.2. Diffusion

Diffusion is the physical process of matter spreading from a region of higher concentration to a region of lower concentration. Examples include the spreading of cream in a cup of coffee and the deflation of a helium balloon over time. In more general terms, diffusion may refer not only to the movement of matter but also of heat. For example, if one end of a block is heated rapidly and then the heat source is removed, over time the heat will diffuse through the block until the temperature of the block becomes uniform [20].

Diffusion can also be defined as the process where an initially non uniform distribution of species in a mixture proceeds toward uniform distribution [16]. It is usually illustrated by the classical experiment in which a tall cylindrical vessel has its lower part filled with iodine solution, for example, and a column of clear water is poured on top, carefully and slowly, so that no convection currents are set up. At first the colored part is separated from the clear by a sharp, well-defined boundary. Later it is found that the upper part becomes colored, the color getting fainter towards the top, while the lower part becomes correspondingly less intensely colored. After sufficient time the whole solution appears uniformly colored. There is evidently therefore a transfer of iodine molecules from the lower to the upper part of the vessel taking place in the absence of convection currents. The iodine is said to have diffused into the water [14, 15].

2.2.1. The theoretical basis of diffusion

Atoms and molecules are constantly in motion. Each atom or molecule undergoes many collisions with others in the gas or liquid in a very short period of time. Because of this, the atom or molecule appears to move in a somewhat random fashion, as illustrated in fig1. This motion is often referred to as a random walk [16]. If it were possible to watch individual molecules of iodine when it diffused into water, it would be found that the motion of each molecule is a random one. In a dilute solution each molecule of iodine behaves independently of the others, which it seldom meets, and each is constantly undergoing collision with solvent molecules, as a result of which collisions it moves sometimes towards a region of higher, sometimes of lower, concentration, having no preferred direction of motion towards one or the other. The motion of a single molecule can be described in terms of the familiar 'random walk' picture, and whilst it is possible to calculate the mean-square distance traveled in a given interval of time it is not possible to say in what direction a given molecule will move in that time.

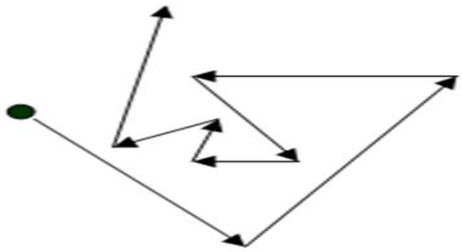

Fig 1:- The motions of molecules or atoms appear to be random walk [15].

This picture of random molecular motions, in which no molecule has a preferred direction of motion, has to be reconciled with the fact that a transfer of iodine molecules from the region of higher to that of lower concentration is nevertheless observed. Consider any horizontal section in the solution and two thin, equal, elements of volume one just below and one just above the section. Though it is not possible to say which way any particular iodine molecule will move in a given interval of time, it can be said that on the average a definite fraction of the molecules in the lower element of volume will cross the section from below, and the same fraction of molecules in the upper element will cross the section from above, in a given time. Thus, simply because there are more iodine molecules in the lower element than in the upper one, there is a net transfer from the lower to the upper side of the section as a result of random molecular motions [15].

2.2.2. Basic hypothesis of mathematical theory of diffusion

Transfer of heat by conduction like diffusion is a random process in which from one part to another by random molecular motions and there is an obvious analogy between the two processes. This was recognized by Fick's (1855), who first put diffusion on a quantitative basis by adopting the mathematical equation of heat conduction derived some years earlier by Fourier (1822). The mathematical theory of diffusion in isotropic substances is therefore based on the hypothesis that the rate of transfer of diffusing substance through unit area of a section is proportional to the concentration gradient measured normal to the section [15, 21].

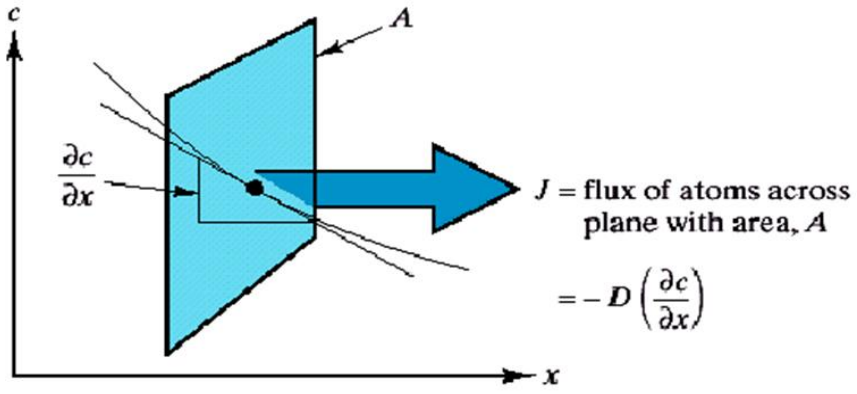

Fig 2:- the rate of transfer of diffusing of atoms per unit area of section [15, 21].

$$J = -D \frac{\partial c}{\partial x} \tag{2}$$

The negative sign arises diffusion occurs in the direction opposite to that of concentration. Where:- J is the rate of transfer per unit area of section, c - concentration of diffusing substance, x - the space coordinate measured normal to the section, D- the diffusion coefficient. In some cases e.g. Diffusion in dilute solution (D) can reasonably be taken as a constant, while in other diffusion (in high polymers), it depends very markedly on concentration. If the amount of material diffusing (J) and the concentration(c) are both expressed in terms of the same unit of quantity, gram/gram molecules, then, D is independent of this unit and has dimensions $(\text{length})^2(\text{time})^{-1}$.

2.2.3. Differential equation of diffusion

The fundamental differential equation of diffusion in an isotropic medium is derived from Eq.2 as follows. Consider an element of volume in the form of a rectangular parallelepiped whose sides are parallel to the axes of coordinates and are of lengths 2dx, 2dy, 2dz. Let the center of the element be at $P(x, y, z)$, where the concentration of diffusing substance is C. Let ABCD and A'B'C'D' be the faces perpendicular to the axis of x as in figure 3. Then the rate at which diffusing substance enters the element through the face ABCD in the plane $x - dx$ is given by:

$$4dydz(Fx - \frac{\partial Fx}{\partial x}dx) \quad (3)$$

Where: - Fx is the rate of transfer through unit area of the corresponding plane through P. Similarly, the rate of loss of diffusing substance through the face A'B'C'D' is given by:

$$4dydz(Fx + \frac{\partial Fx}{\partial x}dx) \quad (4)$$

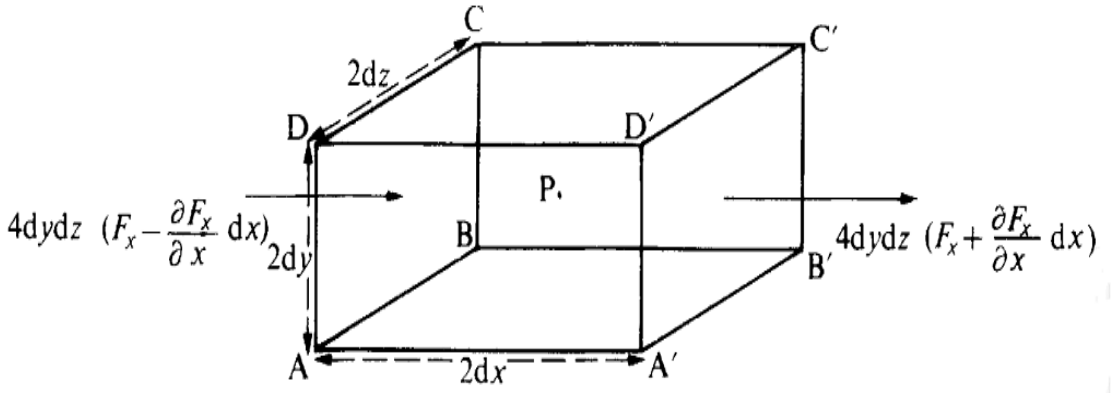

Fig 3:- Element of Volume [14].

The contribution to the rate of increase of diffusing substance in the volume element from these two faces is thus equal to

$$-8dxdydz(\frac{\partial Fx}{\partial t})$$

Similarly, from the other faces we obtain

$$-8dxdydz(\frac{\partial Fy}{\partial t}) \quad \text{And} \quad -8dxdydz(\frac{\partial Fz}{\partial t})$$

But the rate at which the amount of diffusing substance in the element increases is also given by

$$-8dxdydz(\frac{\partial C}{\partial t}) \quad (5)$$

And hence we have immediately

$$\frac{\partial \mathrm{C}}{\partial \mathrm{t}} + \frac{\partial \mathrm{Fx}}{\partial \mathrm{x}} + \frac{\partial \mathrm{Fy}}{\partial \mathrm{y}} + \frac{\partial \mathrm{Fz}}{\partial \mathrm{z}} = 0 \quad (6)$$

If the diffusion coefficient is constant, Fx, Fy, Fz are given by (2) and (6) becomes

$$\frac{\partial C}{\partial t} = \left[\frac{(\partial c^2)}{(\partial x^2)} + \frac{(\partial c^2)}{(\partial y^2)} + \frac{(\partial c^2)}{(\partial z^2)}\right] \quad (7)$$

And equation (7) reduces to

$$\frac{\partial C}{\partial t} = D\left[\frac{(\partial c^2)}{(\partial x^2)}\right] \quad (8)$$

2.2.4. The empirical laws of diffusion

The phenomenological description of diffusion is embodied in Fick's two laws, which are empirical statements that relate the diffusive flow of matter to concentration gradients. To illustrate these laws, consider a single-phase dilute binary alloy in which the constituents are in homogeneously distributed and let c be the concentration of the minor constituent. The concentration is function of position and time and the concentration gradient induces a flow of matter [15, 16].

Fick's First law: - States that "The flux of the diffusing species in a given direction has a magnitude proportional to the concentration gradient in that direction".
That is, if J_1 is the flux along the x_1 axis, then

$$\vec{J}_1 = -\vec{D}_1 \frac{\partial \vec{c}}{\partial x_1} \quad (9)$$

Where: - D_1 is proportionality factor called diffusion coefficient.
The negative sign expresses the fact that diffusion occurs from the region of high concentration to region of low concentration [22].If points in a Cartesian coordinate system with unit vectors (i_1, i_2, i_3), then we would expect that an equation similar to Eq.3 hold for each of the three directions along the coordinate axis.

For Isotropic systems such as gases and liquids, this turns out to be the case. Furthermore, for such systems the diffusing coefficient is experimentally found to be the same in all directions. In nonhomogeneous systems, however it is not the same in all directions. Also the flux in one direction can depend on the flux in the other direction [14].

These results can be described by a generalized Fick's first law, as

$$\vec{J}_1 = \vec{D}_{11}\frac{\partial \vec{c}}{\partial x_1} - \vec{D}_{12}\frac{\partial \vec{c}}{\partial x_2} - \vec{D}_{13}\frac{\partial \vec{c}}{\partial x_3} \tag{10}$$

Similarly the fluxes in other two directions of the Cartesian coordinate system are given by

$$\vec{J}_2 = \vec{D}_{21}\frac{\partial \vec{c}}{\partial x_1} - \vec{D}_{22}\frac{\partial \vec{c}}{\partial x_2} - \vec{D}_{23}\frac{\partial \vec{c}}{\partial x_3} \tag{11}$$

$$\vec{J}_3 = \vec{D}_{31}\frac{\partial \vec{c}}{\partial x_1} - \vec{D}_{32}\frac{\partial \vec{c}}{\partial x_2} - \vec{D}_{33}\frac{\partial \vec{c}}{\partial x_3} \tag{12}$$

These equations can be written in a compact form by defining the flux vector J as

$$\vec{J} = \vec{J}_1 i_1 + \vec{J}_2 i_2 + \vec{J}_3 i_3 \tag{13}$$

And the diffusion dyadic D

$$\vec{D} = \vec{D}_{11} i_1 i_1 + \vec{D}_{12} i_1 i_2 + \vec{D}_{13} i_1 i_3 + \vec{D}_{21} i_2 i_1 + \vec{D}_{22} i_2 i_2 + \vec{D}_{23} i_2 i_3 + \vec{D}_{31} i_3 i_1 + \vec{D}_{32} i_3 i_2 + \vec{D}_{33} i_3 i_3 \tag{14}$$

The equation ref.3-6 give the generalized **Fick's First law** as

$$\vec{J} = -\vec{D}\nabla\vec{c} \tag{15}$$

Fick's Second law: - states that "The time rate of change of concentration in volume element of membrane with in the differential filed is proportional to the rate of change of flux gradient at that point in the field." i.e.

$$\frac{\partial \vec{c}}{\partial t} + \overrightarrow{\nabla} \cdot \vec{J} = 0 \tag{16}$$

This is just an expression of law of conservation of matter and states that, any change in concentration in a volume element is the result of the difference in matter flow in and out of the volume element [16, 22].

Combining equations 15 and 16 gives a generalized form of **Fick's second law**:-

$$\frac{\partial \vec{c}}{\partial t} = \nabla \overrightarrow{D}. \nabla \vec{c} \tag{17}$$

In Isotropic and cubic systems this takes a particularly simple form since $\vec{D}_1 = \vec{D}_2 = \vec{D}_3 = \vec{D}$ [16, 23]. If $\vec{D}$ is a constant independent of position and time the simplification is even greater and Fick's laws become:-

$$\frac{\partial \vec{c}}{\partial t} = \vec{D}(\nabla^2 \vec{c}) \tag{18}$$

2.2.5. Diffusion coefficient and mean free path

The average distance an atom or a molecule travels between collisions is called its mean free path. The mean free path depends upon the size of the atom or molecule. For typically small molecule in the gas phase at 300K, the mean free path is about 8mm. Taking an average speed of 400m/s the average time of collisions is about 2×10^{-10} m^2/sec, this means that small molecules makes 5×10^9 collisions per second. As the molecules undergo this seemingly random motion induced by collisions with other atoms or molecules they migrate through the solution. If there are initially larger proportions of molecules of particular type in one region of the solution, then over the time the molecules will spread out and become evenly distributed throughout the solution. This is the process of diffusion for an initial concentration gradient of a gas or liquid media. The rate at which the molecules spread out is proportional to the difference in the concentration gradient. [15, 20]

$$\text{Rate of Diffusion} = \vec{D} \times \text{Concentration gradient} \quad (19)$$

Where: - D is diffusion coefficient gradient in (length) ^{2}/time. It is a measure of the number of molecules moving through a particular cross-sectional area per unit of time. Experimental measurement of typical diffusion coefficient in water at 300K yields values in the range of 10^{-6}cm^2/s. Diffusion coefficient is related to the mean free path that a molecule travels via **Einstein-Smoluchowsky** equation.

$$\vec{D} = \frac{\lambda^2}{2\tau} \quad (20)$$

Where: - λ - is the mean free path, τ - average time between collisions. Assuming that the average time between the collisions can be calculated from the average speed and mean free path, the time between the collisions can be expressed as

$$\tau = \frac{\lambda}{v_{ave}} \quad (21)$$

Where: - v_{ave} is the average speed of molecule.
Combining Eq.20 and 21 gives

$$\vec{D} = \frac{\lambda v_{ave}}{2} \quad (22)$$

Using the gas phase value of 80nm for the mean free path and 400m/s as the average speed the predicated diffusion coefficient for a small molecule is 1.6 ×10^{-6}m^2/s, which is much larger than the typical value for the diffusion coefficient of liquid phase 10^{-9}m^2[24, 25].

2.2.6. Diffusion coefficient and viscosity

The transport property which is most important for the fluid to flow is the Viscosity. Viscous forces appear only when adjacent part of fluid is moving with different velocities. Thus in the flow of liquid down a pipe the liquid layer which is usually in contact with the pipe is stationary and the axial region is moving with maximum velocity. Common

experience is that high viscosity liquid will flow more slowly than a low viscosity liquid, like water for a given applied pressure difference. **Poiseuille's** formula for the flow of liquid in a capillary of radius R and length l is

$$\frac{dV}{dt} = \frac{({P_1}^2 - {P_0}^2)\pi R^4}{16\eta\, P_0\, l} \tag{23}$$

Where:-V is the volume of flowing fluid, P_1 and P_0, are the pressure at each end of the tube, l is the length of the tube and η - is the coefficient of viscosity [20]. Diffusion in the fluid medium is related to a measurable property called viscosity. Viscosity is the measure of the resistance to the fluid flow. Liquid such as water that flow easily have a relatively low viscosity compered to thicker fluids. The viscosity of liquid is also its measure to transport momentum. Its unit is poise (P). Where 1P = 0.1Kg/m. s. Typical viscosities are in the range of 10^{-4}P for gas and 10^{-2}P for liquids. Kinetic theory of gas predicts that viscosity is independent of pressure and proportional to the square root of the absolute temperature. For liquid viscosities have an exponential dependence on the temperature as described by the formula:

$$\eta = Aexp^{\frac{[\Delta E_v]}{RT}} \tag{24}$$

Where:-ΔE_V-an activation barrier. R-is the radius of the molecule. T -is the temperature. The relation between diffusion coefficient and viscosity is given by **Einstein-Stokes** equation

$$\vec{D} = \frac{KT}{6\pi\eta R} \tag{25}$$

Where: K-is Boltzmann's constant. T -temperature. R-is the radius of the molecule.
The equation is derived, of course, assuming that the molecule is spherical in shape. The Einstein-Stokes equation shows that the viscosity and diffusion coefficient are inversely related.

D_0 is also related to temperature via the equation [20, 25].

$$\vec{D} = \vec{D}_0 exp^{\frac{[-E_A]}{RT}} \quad (26)$$

Where: - D_0 -is the diffusion coefficient at infinite temperature (maximum diffusion coefficient). E_A -is activation energy

2.2.7. Random walk as a statistical model for diffusion (One-dimensional treatment)

Process such as diffusion in which a single molecule moves through a solution of huge number of particles, can be models statically. Even though the presence of other particles can affect the dynamics of the particle of interest through collision and interactions we can consider the motion of particle as a random walk. The diffusion as a motion of random walk simulation can be shown by calculating the average square distance from the origin. To do this, many individual walks simulation is carried out, and the average is taken over many individual walks. Let us consider a distribution where the concentration depends on only one coordinate, be the x-coordinate (one - dimensional diffusion). The concentration of the marked (atom) particle is then as a function of position (x) and time ($'t'$). Let it be c (x, t). In order to calculate, the diffusion flow we need to count the number of particles which pass through a surface of unit area, perpendicular to the axis, in the plane x_0 during time (t) [26].

The particles migrate through the lattice by making a sequence of jumps owing to the presence of defects. We have chosen the case of tracer-diffusion with no external applied force, so that the probability of displacement is the same along both positive and negative direction and it will be called x. Let us define the distribution function $f(x, t)\, dt$ as the probability of displacement with a projection between x and $x + dx$.
It follows from this definition that

$$\int_{-\infty}^{\infty} f(x,t)dx = 1 \quad (27)$$

More over since they jumps along both + x and - x direction occur with the same probability one has

$$f(x,t) = f(-x,t) \tag{28}$$

Considering a large number of particles the projection of the mean displacement $<x>$ may then be written as [20, 27]

$$< x >= \int_{-\infty}^{\infty} x\, f(x,t)dx \tag{29}$$

It follows from Eq.28 and every $< x^{2n+1} >$ is zero. The most important parameter in diffusion is the mean square displacement, $< x^2 >$ the projection of which is then:

$$< x^2 >= \int_{-\infty}^{\infty} x^2 f(x,t)\mathrm{d}x \tag{30}$$

Results for $< x^2 >$ versus time for a random walk of one dimension is shown in fig.4 below

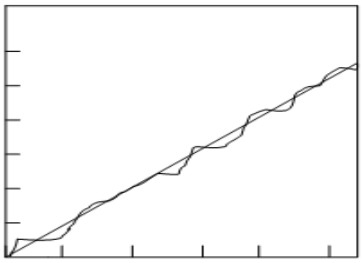

Fig 4:- Diffusion and random motion. [26]

The result presented on the figure shows that the system follows equation

$$< x^2 > \ \propto \mathrm{D} \cdot \mathrm{t} \tag{31}$$

Where: - t - is the time (proportional to the number of steps)

D - Is the diffusion coefficient

2.3. Moiré pattern and moiré defelectometry

2.3.1 Interference of fringes on screen

Interference is a matter of common experience that two trains of ripple on the surface of water cross each other and proceed onward in their direction undisturbed. In the same way two beams of light cross each other and proceed without being influenced by each other in any way. However in the region of crossing where both beams are acting simultaneously, we expect modification in their intensity which should be either less or greater than that which would be given by one beam alone. This modification of intensity due to superposition of two or more beams of light is interference of light [28].

2.3.1.1 Theory of interference

We shall now derive an expression for the resultant intensity at any point P on the screen due to superposition of two waves of light having equal amplitude, equal wave length and equal velocity but initially stating with constant phase difference [23, 28]. Illuminate slits S_1 and S_2 with monochromatic light of wave length λ. The slits to be equidistant from S_1 and S_2, the other slits. As a consequence waves of light from S always arrive at S_1 and S_2 is equal phase and at any instant time't'. We may there represent by the equation:

$$Y = a \sin(\frac{2\pi t}{T}) \quad (32)$$

Where: - a- amplitude, T- period of simple periodic vibration.

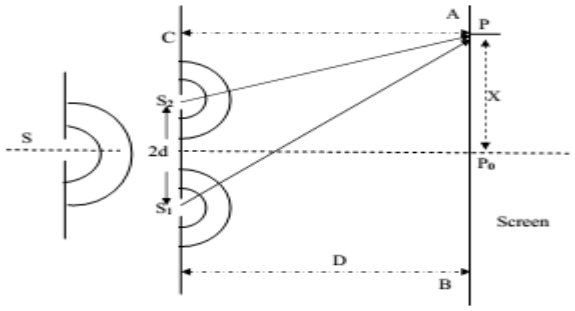

Fig 5:- Interference of monochromatic light [23]

In travelling from S_1 to P the phase of wave alter by $2\pi(\frac{S_1P}{\lambda})$. Hence at the instant time't', the liner displacement at P due to this wave will be expressed by

$$Y_1 = a \sin 2\pi[\left(\frac{t}{T}\right) - (\frac{S_1P}{\lambda})] \quad (33)$$

Similarly at the instant time 't' the displacement of P due to vibration of light from S_2 will be represented by

$$Y_2 = a \sin 2\pi[\left(\frac{t}{T}\right) - (\frac{S_2P}{\lambda})] \quad (34)$$

According to the principle of superposition of wave motion, the resultant displacement is given by

$$Y = Y_1 + Y_2 \quad (35)$$

$$Y = a \sin 2\pi[\left(\frac{t}{T}\right) - (\frac{S_1P}{\lambda})] + a \sin 2\pi[\left(\frac{t}{T}\right) - (\frac{S_2P}{\lambda})] \quad (36)$$

Let $S_1P = \alpha$ and $S_2P = \Delta + \alpha$ where $\Delta = S_2P - S_1P$ is called the optical path difference between the two superposed waves at P we may now write,

$$Y = a \sin 2\pi[\left(\frac{t}{T}\right) - (\frac{\alpha}{\lambda})] + a \sin 2\pi[\left(\frac{t}{T}\right) - (\frac{\alpha+\Delta}{\lambda})] \quad (37)$$

$$Y = 2a \cos\frac{\Delta\pi}{\lambda} \sin [\left(\frac{t}{T}\right) - (\frac{\alpha+\frac{\Delta}{2}}{\lambda})] \quad (38)$$

A wave of the same wave length and period as the component of waves but with amplitude

$$R = 2a \cos (\frac{\Delta\pi}{\lambda}) \quad (39)$$

Which varies between 0 and 2a with proper variation in the magnitude of Δ. Also if δ is the phase difference corresponding to the path difference Δ between the two superposed waves at point p then

$$\delta = \frac{2\pi\Delta}{\lambda} = \frac{2\pi}{\lambda}(S_2P - S_1P) \tag{40}$$

The resultant amplitude R can now be expressed in the form

$$R = 2a\cos\frac{\pi\Delta}{\lambda} = 2a\cos\frac{1}{2}\left(\frac{2\Delta\pi}{\lambda}\right) = 2a\cos\left(\frac{\delta}{2}\right) \tag{41}$$

The resultant intensity I at point P is proportional to the square of the amplitude R, and hence we can write I proportional to $4a^2\cos^2\left(\frac{\delta}{2}\right)$ assuming that the constant of proportionality to be unity, for simplicity it can be easily expressed as

$$I = 2a^2(1 + \cos\delta) \tag{42}$$

Which varies with the magnitude of δ.

In order to plot the intensity distribution in the interference pattern arising from the interference of light waves from two coherent sources S_1 and S_2 it is essential to investigate the spacing of these fringes on the screen placed parallel to the line joining S_1 and S_2.At any point P on the screen the resultant intensity is maximum or minimum according as its distance from two coherent sources S_1 and S_2 which always in equal phase difference exactly by even or odd multiple of $\frac{\lambda}{2}$,where λ the wave length of the light emitted by the sources [28, 29]. In symbols the conditions are expressed as

$$S_2P - S_1P = \frac{2n\lambda}{2} \qquad \text{(Bright Fringes)} \tag{43}$$

$$S_2P - S_1P = \frac{(2n+1)\lambda}{2} \qquad \text{(Dark Fringes)} \tag{44}$$

2.3.2. Diffraction

According to geometrical optics, if an opaque object is placed between a point light source and screen, the edges of the object will cast a sharp shadow on the screen (the penumbra will be negligible) if the source is sufficiently small, no light will reach the screen at points with in the geometrical shadow, while outside the shadow the screen will be uniformly illuminated. A small amount of light has "bent" around the edges into the geometrical shadow which is broadened by alternate bright and dark bands. In the first bright band outside the geometrical shadow, the illumination is actually greater than in the region of uniform illumination at the extreme left. The term diffraction applied to problems such as this one is concerned with the resultant effect produced by a limited portion of a wave front. Since in most diffraction problems some light is found within the region of geometrical shadow, diffraction is sometimes defined as the bending of light around an obstacle [28, 30].

2.3.2.1. The plane diffraction grating

An arrangement consisting of large number of slits of the same width and separated by equal opaque spaces is known as diffraction grating. This was first constructed by Joseph Fraunhhofer and it was due to this study of diffraction of parallel beams of light by grating in 1819 that his name become associated with this class of diffraction phenomena. The diffraction pattern suffers a modification as the number of slits is increased beyond two [23, 31].

2.3.3 Moiré and fringe projection techniques

The term moiré is a French word, which refers to "an irregular wavy finish usually produced on a fabric by pressing between engraved rollers". In optics it refers to a pattern produced between two gratings of approximately equal spacing. It can be seen in everyday things such as the overlapping of two window screens, the recreating of half-tone picture, or with striped shirt seen on television.

The use of moiré for reduce sensitive testing was introduced by Lord Rayleigh in 1874. He looked at the moiré between two identical gratings to determine their quality even though each individual gratings could not be resolved under a microscope [17, 27, and 32].Fringe projection entails projecting a fringe pattern or grating on an object and viewing it from a different direction. The first use of fringe projection for determining surface topography was presented by Row and Welford in 1967. It is convenient technique for contouring objects that are too coarse to be measured with standard interferometry.

Fringe projection is related to optical triangulation using a single point of light and light sectioning where a single line is projected onto an object and viewed in different direction to determine the surface contour. Moiré fringe projection interferometry complement conventional holographic interferometry, especially for testing optics to be used at long wave-lengths. Although two-wave length holography (TWH) can be used to contour surface at any longer-than visible wavelength, visible interferometric environmental conditions are required.

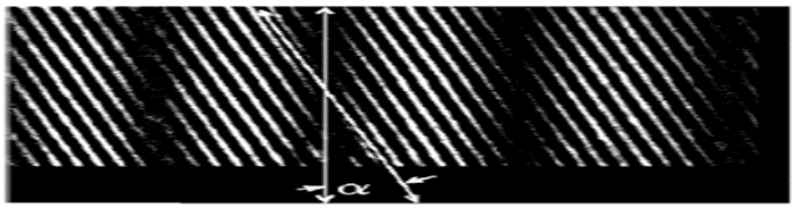

Fig 6:- Moiré fringes at small angle tilt [32]

2.3.3.1 What is Moiré pattern?

Moiré patterns are extremely useful to understand basic interferometry and interferometric test results. The moiré pattern (or beat pattern) produced by two identical straight-line gratings rotated by a small angle relative to each other. A dark fringe is produced when the dark lines are out of step one- half period, and a bright fringe is produced when dark lines of one grating fall on top of the corresponding dark lines of the second grating. If the angle between the two gratings is increased, the separation between the bright and dark fringes decreases. [15, 17, 32].

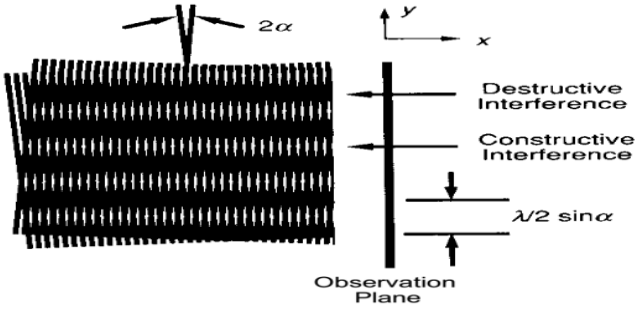

Fig 7:- Moiré between two straight-line gratings of the same pitch at angle 2α with respect to each other [15,17and 33].

The following analysis shows how to calculate the moiré pattern for arbitrary gratings. Let the intensity transmission function for two gratings $f_1(x, y)$ and $f_2(x, y)$ be given by

$$f_1(x,y) = a_1 + \sum_{n=1}^{\infty} b_{1n} cos\lfloor n\phi_1(x,y)\rfloor \quad (45)$$

$$f_2(x,y) = a_2 + \sum_{n=1}^{\infty} b_{2m} cos\lfloor n\phi_1(x,y)\rfloor \quad (46)$$

Where $\phi(x, y)$ is the function describing the basic shape of the gratings lines.

For the fundamental frequency,

$\phi(x, y) = 2n\pi$ at the center of each bright line

And is equal to an integer plus one-half times π,

$\phi(x, y) = 2\pi(n + \frac{1}{2})$ at the center of each dark line.

The coefficient b determine the profile of the grating lines (i.e., square wave triangular, sinusoidal, etc.) For a sinusoidal line profile, b_{i1} is only non-zero term. When these two gratings are superimposed, the resulting intensity transmission function is given by the product

$$f_1(x,y)f_2(x,y) = a_1a_2 + a_1\sum_{m=1}^{\infty} b_{2m} cos\lfloor m\phi_2(x,y)\rfloor + a_2\sum_{n=1}^{\infty} b_{1n} cos\lfloor n\phi_1(x,y)\rfloor + \sum_{n=1}^{\infty}\sum_{m=1}^{\infty} b_{2m}b_{1n} cos\lfloor n\phi_1(x,y)\rfloor cos\lfloor m\phi_2(x,y)\rfloor \quad (47)$$

The first three terms of Eq.47 provide information that can be determined by looking at the two patterns separately; but the last term contains information about the relationships. It can be written as follows

$$\sum_{n=1}^{\infty}\sum_{m=1}^{\infty} b_{1n}b_{2m}cos\lfloor n\phi_1(x,y)\rfloor cos\lfloor m\phi_2(x,y)\rfloor =$$

$$\frac{1}{2}b_{12}b_{21}\cos[\phi_1(x,y)-\phi_2(x,y)] +$$

$$\frac{1}{2}\sum_{n=1}^{\infty}\sum_{m=1}^{\infty} cos[n\phi_1(x,y)-m\phi_2(x,y)] +$$

$$\frac{1}{2}\sum_{n=1}^{\infty}\sum_{m=1}^{\infty} b_{1n}b_{2m}cos[n\phi_1(x,y)+m\phi_2(x,y)] \quad (48)$$

This expression shows that by superimposing the two gratings, the sum and difference between two gratings is obtained. The first term of Eq.48 represents the difference between the fundamental pattern masking up the two gratings. It can be used to predict the moiré pattern in **fig 7**, assuming that two grating are oriented with an angle 2α between them with the y-axis of coordinate system bisecting this angle as shown in **fig 7**.

Then the two grating functions $\phi_1(x, y)$ and $\phi_2(x, y)$ can be written as

$$\phi_1(x,y) = \frac{2\pi}{\lambda_1}(x\cos\alpha + y\sin\alpha) \quad (49)$$

$$\phi_2(x,y) = \frac{2\pi}{\lambda_2}(x\cos\alpha - y\sin\alpha) \quad (50)$$

Where λ_1 and λ_2 are line spacing of the two gratings. Eq.49 and Eq.50 can be written as

$$\phi_1(x,y) - \Phi_2(x,y) = \frac{2\pi}{\lambda_{beat}}x\cos(\alpha) + \frac{4\pi}{\lambda_{ave}}y\sin\alpha \quad (51)$$

Where λ_{ave} is the average line spacing, λ_{beat} is the beat wave length between the two gratings given by

$$\lambda_{beat} = \frac{\lambda_1\lambda_2}{\lambda_2-\lambda_1} \quad (52)$$

$$\lambda_{ave} = \frac{\lambda_1\lambda_2}{\lambda_2+\lambda_1} \quad (53)$$

Note that this beat wavelength equation is the same as that obtained for two wavelength interferometry in Eq.48, the moiré or beat will be lines whose centers satisfy the equation

$$\phi_1(x,y) - \phi_2(x,y) = M\,2\pi \tag{54}$$

Three separate cases for moiré fringe can be considered [15, 34].

[1].When $\lambda_1 = \lambda_2 = \lambda$ the first term of Eq.51 is zero, and the fringe center are given by

$$M\lambda = 2y \sin\alpha \tag{55}$$

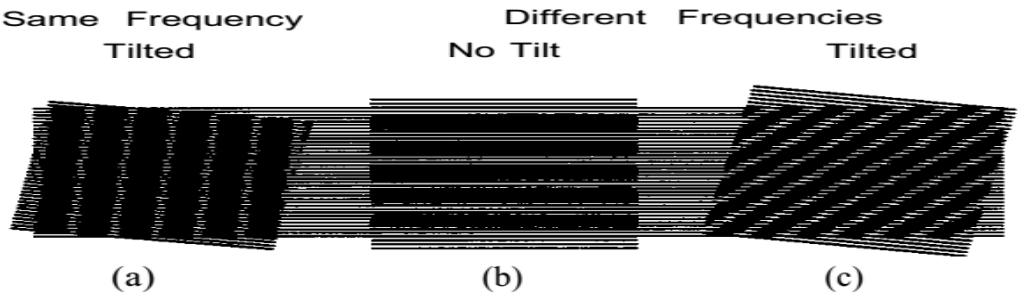

Fig 8:- Moiré pattern caused by two straight-line gratings [15, 34]:-

(a) The same pitch tilted with respect to one another,

(b) Different frequencies and no tilt, and (c) Different frequencies tilted with respect to one another.

Where M is an integer corresponding to the fringe order. As we expected, Eq.54 is the equation of equal-spaced horizontal lines as seen in **fig 8**.

[2].The other simple case occurs when the gratings are parallel to each other with $\alpha = 0$.This makes the second term of Eq.51, the Moiré will be line that satisfy

$$M\lambda_{beat} = x \tag{56}$$

These fringes are equally spaced, vertical lines parallel to the y-axis.

[3].For the more general case where two gratings have different line spacing and the angle between the gratings is nonzero, the equation will now be

$$M\lambda_{ave} = \frac{\lambda_{ave}}{\lambda_{beat}} x\cos\alpha + 2y\sin\alpha \tag{57}$$

This is the equation of straight lines whose spacing and orientation depends on the relative difference between two grating spacing's and the angle between the gratings. **Fig 8**. Shows Moiré patterns for these three cases. The orientation and spacing of the moiré fringes for the general case can be determined by the geometry shown in **fig 9**. The distance $\overline{AB}$ can be written in terms of the two grating spacing's:

$$\overline{AB} = \frac{\lambda_1}{sine(\theta-\alpha)} = \frac{\lambda_2}{sine(\theta+\alpha)} \tag{58}$$

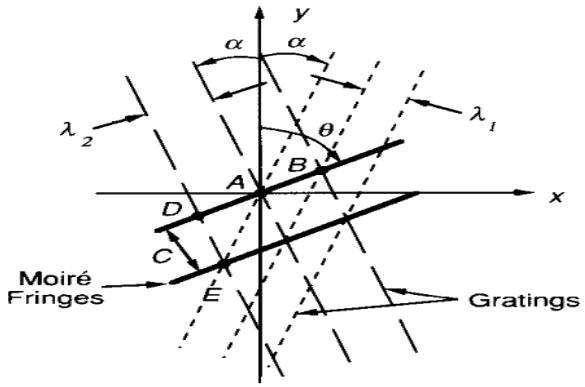

Fig 9:- Geometry used to determine spacing and angle between two gratings of different frequencies [15, 34]

Where θ is the angle the Moiré fringes make with the y-axis. After rearranging the fringe orientation angle θ is given by

$$\tan\theta = \tan\alpha\left(\frac{\lambda_1+\lambda_2}{\lambda_2-\lambda_1}\right) \tag{59}$$

When $\alpha = 0$ and $\lambda_1 \neq \lambda_2$, $\theta = 90^0$ and when $\lambda_1 = \lambda_2$ with $\alpha \neq 0$ $\theta = 90^0$ as expected. The fringe spacing perpendicular to the fringe lines can be found by equating quantities for the distance $\overline{DE}$

$$\overline{\mathrm{DE}} = \frac{\lambda_1}{sin2\alpha} = \frac{C}{sin(\theta+\alpha)} \tag{60}$$

Where C is the fringe spacing or contour interval. This can be rearranged to yield

$$C = \lambda_1 [\frac{sin(\theta+\alpha)}{sin2\alpha}] \quad (61)$$

By substituting for the fringe orientation θ, the fringe spacing can be found in terms of the grating spacing and angle between the gratings:

$$C = [\frac{\lambda_1 \lambda_2}{\sqrt{\lambda_1{}^2 sin^2 2\alpha + (\lambda_2 cos2\alpha - \lambda_1)^2}}] \quad (62)$$

In the limit that $\alpha = 0$ and $\lambda_1 \neq \lambda_2$, the fringe space equals λ_{beat}, and in the limit that $\lambda = \lambda_1 = \lambda_2$ and $\alpha \neq 0$, the fringe space equals $\frac{\lambda}{2}\sin \alpha$. It is possible to determine λ_2 and α, from the measured fringe spacing and orientation as long as λ_1 is known.

2.3.3.2. Fringe projection techniques

A simple approach for contouring is to project interference fringes or grating onto an object and then view from another direction, as shown in **fig 10**. Assuming a collimated illumination beam and viewing the fringe with a telocentric optical system, straight equally spaced fringes are incident on the object, producing equally spaced contour intervals. The departure of a viewed fringe from a straight line shows the departure of the surface from a plane reference surfaces. When the fringes are viewed at an angle α relative to the projection direction, the spacing of lines perpendicular to the viewing direction will be:-

$$d = p \cos \alpha \quad (63)$$

The contour interval C (the height between adjacent contour lines in the viewing direction) is determined by the line or fringe spacing projected onto the surface and the angle between the projection and viewing directions;

$$C = \frac{p}{\sin \alpha} = \frac{d}{\tan\alpha} \tag{64}$$

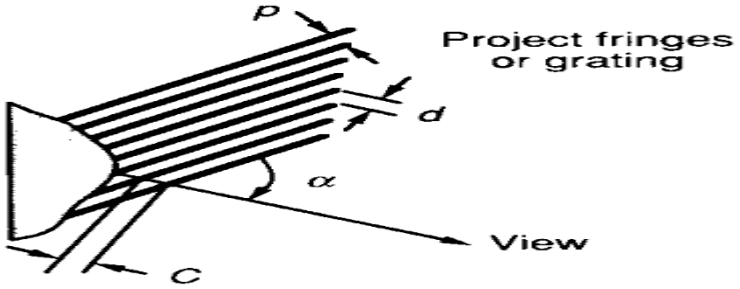

Fig 10:- Projection of fringes or gratings onto an object and observing it at angle α [17, 29].

P is gratings (pitch) and C the contour interval.

These contour lines are planes of equal height, and the sensitivity of the measurement is determined by α. The larger the angle α, the smaller contour interval. If $\alpha = 90^0$, then the counter interval is equal to p, and the sensitivity is maximum. The reference plane will be parallel to the direction of fringes and perpendicular to the viewing direction as shown in **fig.10**. Even though the maximum sensitivity can be obtained at 90^0. When $\alpha = 0$, the counter interval is infinite and the measurement sensitivity is zero. For best results an angle no longer than the largest slope on the surface should be chosen. When the interference fringes are projected onto surface rather than using grating, the fringe spacing P is determined by relation

$$P = \frac{\lambda}{2\sin \Delta\theta} \tag{65}$$

Where λ is the wave length of illumination and 2Δθ is the angle between the two interfering beams. Substituting the expression for P in to Eq.65, the contour interval becomes:-

$$C = \frac{\lambda}{2(\sin \Delta\theta)\sin\alpha} \tag{66}$$

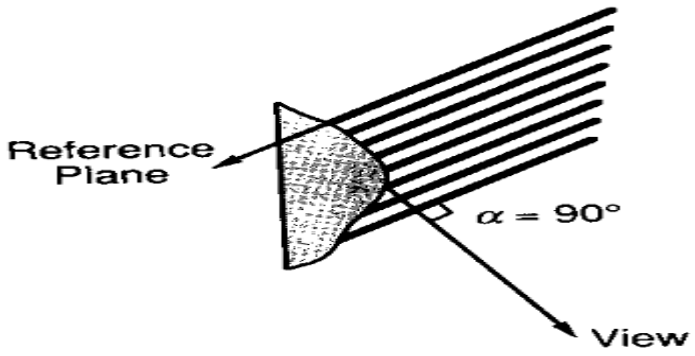

Fig 11:- Maximum sensitivity for fringe projection at 90^0 angle between projection and viewing [17, 29].

Tilting one beam with respect to the other will change the counter interval; the larger the angle between the two beams the smaller the contour interval will be. If the source and the viewer are not at infinity, the fringes or gratings which are projected onto the object will not be composed of straight, equally spaced lines. The height between the contours planes will be a function of the distance from the source and viewer to the object [17, 29, and 34].

2.3.3.3 Shadow Moiré

A simple method form of moiré interferometry for countering objects uses a single grating placed in front of the object as Shown fig 12.The gratings in front of the object produces a shadow on the object that is viewed from different direction through the grating. A low frequency beat or moiré pattern is seen. [27, 33]

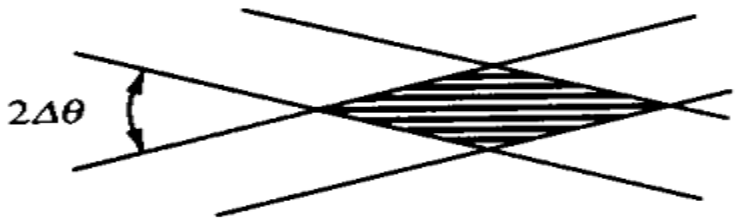

Fig 12:- Fringe produced by two interfering beams [27, 33]

This pattern is due to the interference between the grating shadows on the object and the grating as viewed. Assuming that the illumination is collimated and that the object is viewed at infinity or through a telocentric optical system, the height z between the grating and the object point can be determined from geometry.

This height is given by

$$z = \frac{Np}{(\tan \alpha + \tan \beta)} \tag{67}$$

Where:- α is the illumination angle, β is the viewing angle, p is the spacing of grating lines, and N is the number of grating lines between the points A and B (see in fig13).The contour interval in a direction perpendicular to the grating will simply be given by

$$C = \frac{p}{(\tan \alpha + \tan \beta)} \tag{68}$$

Again, the distance between the moiré fringes in the beat pattern depends on the angle between the illumination and viewing directions. The larger the angle, the smaller the contour interval, the reference plane will be parallel to the grating.

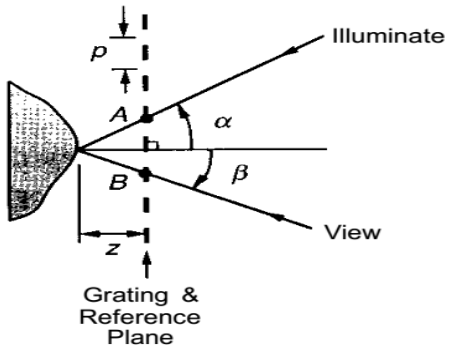

Fig 13:- Geometry for shadow moiré where illumination and viewing points are at infinity [22].

Note that this reference plane is tilted with respect to the reference plane obtained when fringes are projected onto the subject. Essentially the shadow moiré technique provides a way of removing the" tilt" term and repositioning the reference plane. Most of the time, it is difficult to illuminate an entire object with a collimated beam, Therefor, it is important to consider the case of finite illumination and viewing distances. However, for simplicity, only the case where the illumination and viewing positions are the same distance from the

grating will be considered. The grating is assumed to be close enough to the object surface so that the direction effects are negligible. **Fig.** 14 illustrates this phenomenon. [22]
The height between the object and the grating is given by

$$z = \frac{Np}{(\tan \alpha' + \tan \beta')} \tag{69}$$

Where α' and β' are the illumination and viewing angles at the object surface. These

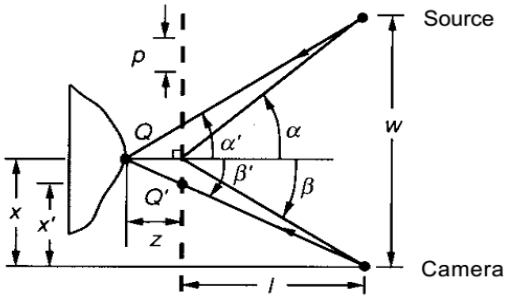

Fig 14: Shadow moiré when both illumination and viewing positions are at finite distances [22].

Angles change for every point on the surface and are different from α and β Where α and β are illumination and viewing angles at the reference surface. The surface height can be written as:

$$z = NC(z) = \frac{Np(l+z)}{\omega} = \frac{Npl}{\omega - Np} \tag{70}$$

This equation shows that the height is complex function depending on the position of the each object point. Thus the distance between contour intervals is dependent on the height of the surface and the number of fringes between the grating and the object. Individual contour lines will no longer be planes of equal height. The expression for height can be simplified by considering the case where the distance to the source and viewer is large compared to the surface height variation, $l >> z$. Then the surface height can be expressed as

$$z = \frac{Npl}{\omega} = \frac{Np}{(\tan \alpha + \tan \beta)} \tag{71}$$

Even though the angles α and β vary from point-to-point on the surface, the sum of their tangents remains equal to $\frac{\omega}{l}$ for the object points as long as $l >> z$. The contour interval will be constant. Because of the finite distances, there is also distortion due to the viewing perspective. A point on the surface Q will appear to be at the location Q' when viewed through the grating. By similarity of triangles, the distances x and x' from the line perpendicular to the grating intersecting the camera location can be related using

$$\frac{x}{z+l} = \frac{x'}{l} \tag{72}$$

$\Rightarrow x = x'(1 + \frac{z}{l})$. Where x represent the actual coordinate in terms of the measured coordinates x'. Similarly the y - coordinate can be corrected as

$$\frac{y}{z+l} = \frac{y'}{l} \tag{73}$$

$\Rightarrow y = y'(1 + \frac{z}{l})$. This enables the measured surface to be mapped to the actual surface to correct the viewing perspective. These same factors can be applied to fringe projection

2.3.3.4 Projection Moiré

Moiré interferometry can also be applied to projecting interfering fringes or grating on to an object and then viewing through a second grating in front of the viewer. The difference between the projection and shadow moiré is that two different gratings are used in the projection moiré. The orientation of the reference frame can be arbitrarily changed using different grating pitch to view the object.

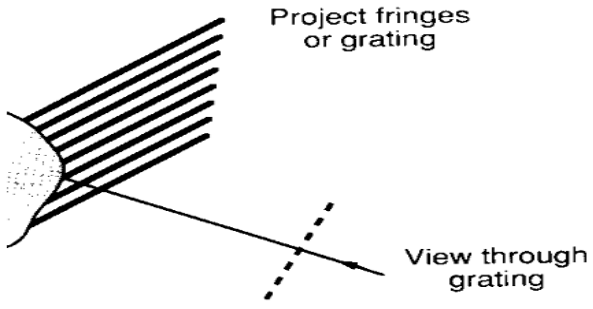

Fig 15:- Projection moiré where fringes or a grating are projected onto a surface and viewed through a second grating [27, 34].

The contour interval can be given by

$$C = \frac{d}{(\tan \alpha + \tan \beta)} \tag{74}$$

Where d is the period of grating in the plane. This makes the projection Moiré the same as shadow moiré although projection moiré can be much more complicated than the shadow moiré [27, 34].

2.3.4. Moiré Defelectrometry

Laser Moiré defelectometry applicable for, mini/micro-scale flow visualization is based on the moiré effect. The displacements of moiré fringes can be used to calculate deflection angle of laser beam, which is induced by the variation of refractive index of thermal flow fluid. The geometry scale less than 1mm is usually called mini/micro-scale. When the conventional optical interferometry (e.g. M-Z interferometry, Holographic interferometry, speckle interferometry etc.) is used, the needs of measurement sensitivity cannot be met because the phase variation produced by mini/micro-scale flow are very small.

In a general way 5-8 interferometry fringes in an interferogram are needed to obtain accurate and reliable experimental data. However, when a light beam passes through the mini/micro-scale flow field, the number of interferometry fringe produced by phase variation of the flow field is often less than one. As a result it is very difficult to extract experimental data from the interferogram; sometimes it is impossible. However when a light beam pass through mini/ micro-scale flow field, the moiré pattern containing more than five fringes can be captured[17, 33].

He-Ne laser is used as a light source for visualization. The expanded and collimated light is formed using an expending lens L_1 (BE) and collimation lens L_2.This parallel collimating beam passes through the flow field to measure and two gratings of amplitude type with the same pitch successively. L_3 is microscopic image lens. Because there is small angle between two gratings forming a series of moiré fringes with the diffractive order (0,

±1, ±2.....) can be formed on image plane of L_3 lens based on the moiré effect. The zero-order moiré fringe is only imaged on the target of CCD by the means of an aperture D. the moiré fringe with information of mini/micro-scale flow are inputting to a micro-computer and are processed to extract the displacement of moiré fringes [21, 27].Suppose that the pitch of both gratings G_1 and G_2 is P and the angle between two gratings formed is θ. The interval between two moiré fringes i.e. spatial period T' of moiré fringes is then given by

$$T' = \frac{P}{\theta} \tag{75}$$

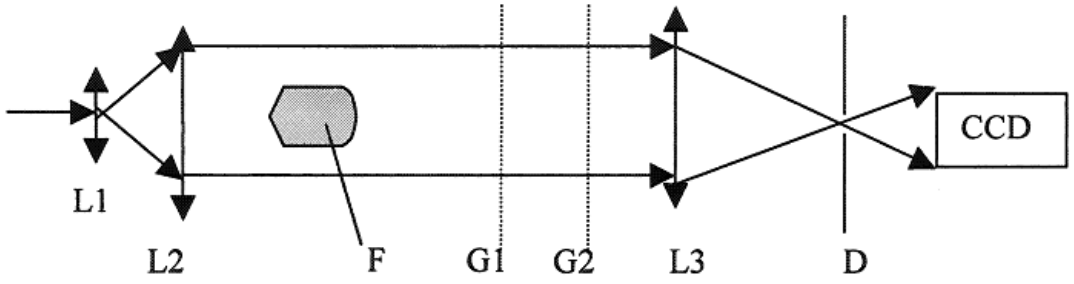

L1− expanding lens L2− collimation lens F−flow field
L3−microscopical image lens G1, G2−gratings D− aperture

Fig16: Experimental arrangement of laser Moiré defelectometery [21, 27].

Correspondingly, its basic spatial frequency f_0 of the moiré fringe is

$$f_0 = \frac{1}{T'} = \frac{\theta}{P} \tag{76}$$

If there is disturbance in flow fluid, the parallel detective light beam deflect after passing through the flow fluid. The deflection angle of light beam is α, the relation between α and displacement h of moiré fringe is given by

$$\alpha = \frac{\theta h}{d} \tag{77}$$

Where d- the distance between two gratings. For a mini/micro-scale flow field, the deflection angle α of the beam is very small, and the corresponding displacement h of the moiré fringe is so small that it is very difficult to measure directly [27, 33]. To improve the measurement accuracy for displacement of moiré fringe, a method by phase

measurement of moiré fringe is proposed. The relation between phase Φ and the displacement h of moiré fringe is

$$\phi = 2\pi f_0 h \tag{78}$$

Thus the deflective angle α can be expressed as

$$\alpha = \frac{\theta h}{\mathrm{d}}$$

But from Eq.77

$$\mathrm{h} = \frac{\phi}{2\pi f_0}$$

$$\alpha = \frac{\theta}{\mathrm{d}}\left[\frac{\phi}{2\pi f_0}\right]$$

From Eq.75

$$P = \frac{\theta}{f_0}$$

$$\alpha = \frac{\phi P}{2\pi d}$$

For a weak deflection, the relation between the deflection angle α and the refractive index n is given by

$$\alpha = \frac{1}{\mathrm{n}_\infty}\int_0^{\mathrm{L}} \frac{\partial \mathrm{n}}{\partial \mathrm{y}}\,\mathrm{dz} \tag{79}$$

Where n_∞-environmental refractive index. L-is the length of test section. Thus, the phase-variation Φ of moiré fringe can be written as the function of refractive index (n)

$$\Phi = \frac{2\pi d}{p\mathrm{n}_\infty}\int_0^{\mathrm{L}} \frac{\partial \mathrm{n}}{\partial \mathrm{y}}\,\mathrm{dz} \tag{80}$$

For a two dimensional flow field, the differential $\frac{\partial \mathrm{n}}{\partial \mathrm{y}}$ of refractive index in y-direction can be obtained a

$$\frac{\partial \mathrm{n}}{\partial \mathrm{y}} = \frac{p\mathrm{n}_\infty \Phi}{2\pi d L} \tag{81}$$

For axis-symmetric flow field, the refractive index $\mathrm{n_r}$ can be written in the following form by means of Abel transform

$$n_r - n_\infty = -\frac{n_\infty \theta}{\pi d} \int_r^\infty \frac{h(x,y)}{\sqrt{y^2 - r^2}} dy \quad (82)$$

$$n_r - n_\infty = -\frac{n_\infty f_0 p}{\pi d} \int_r^\infty \frac{h(x,y)}{\sqrt{y^2 - r^2}} dy \quad (83)$$

or

$$n_r - n_\infty = -\frac{n_\infty p}{2\pi^2 d} \int_r^\infty \frac{h(x,y)}{\sqrt{y^2 - r^2}} dy \quad (84)$$

If a fine grid or grating is illuminated from behind through usually, an identical grid or grating moiré fringes are produced on screen behind the second grid/ grating [35]. Where the imaged moiré fringe is the composite of patterns near grid or grating and the shadow on it of the grid upstream. The nearer grating is undisturbed, but the distortion of the light beam (such as its divergence or convergence) lead to distortion of the shadow component and corresponding distributions in the moiré fringe from their normally regular appearance. The distortion of the light beam could be produced by the presence of simple lens or more interestingly phase object whose optical power varies with position in it such a liquid with density or temperature gradients with in it. Refractive index variations map onto these gradients. The refractive index variations then determines the shape of moiré fringe.

Moiré defelectometery is a wave front technique combining Talbot effect with moiré techniques for measuring and the testing phase objects or refractive surfaces. Moiré deflectograms provided by the light deflection from tested phase objects or refractive surfaces can be used to calculate the deflection angle which represents the refractive index of the phase object or the height of the refractive surface. [15, 27, 35]

2.3.4.1 Phase measuring defelectrometry

This is a new method of defelectometery applied to measure a specular free from surfaces with in few seconds. The basic principle of the technique is to project the sinusoidal fringe patterns on screen located remotely from the surface under test and to observe the fringe reflected via the surface. Any slope variation leads to a distortion pattern. Using well

known phase shifting algorithm, we can precisely measure these distortion and then calculate the surface normal in each pixel [15, 30]. Among the methods for extraction of phase from intentional distribution, Fourier transformer method of computer based fringe pattern analysis is more suitable for the mini or micro-scales flow visualization because a very small displacement of moiré fringes can be obtained. The mathematical model for extraction of phase from intensity distribution of moiré fringe is as follows. The intensity distribution I (x, y) of moiré fringe can be expressed as:

$$I(x,y) = \mathrm{a}(x,y) + b(x,y)\cos[2\pi f_0 x + \phi(x,y)] \tag{85}$$

Where $\Phi\ (x, y)$ is the phase that contains useful information and a (x, y) and b (x, y) are intensity factors which results from propagation of light beam. In order to extract the phase Eq.85 transformed into the following form by:

$$e^{ix} = cosx + isinx\ .$$

$$I(x,y) = \mathrm{a}(x,y) + C(x,y)e^{(i2\pi f_0 x)} + C_{ave}(x,y)e^{(-i2\pi f_0 x)}] \tag{86}$$

Where

$$C(x,y) = \frac{1}{2}b(x,y)e^{(i\phi(x,y))} \text{ and } C_{ave}(x,y) = \frac{1}{2}b^* e^{(-i\phi(x,y))}$$

By using one-dimensional Fourier transformer for x-coordinate Eq.84 transfer

$$I(x,y) = A(f,y) + C(f - f_0, y) + C_{ave}(f + f_0, y) \tag{87}$$

Where f is the spatial frequency in x co-ordinate. Eq.86 expresses function of frequency distribution corresponding to Eq.85.The capital letters are the coefficient of Fourier transform. In order to extract the phase factor from the spatial frequency distribution, a band pass filter is used. As a result, the term $C(f - f_0, y)$ is kept only. The expression of Fourier inverse transformation for the term $C(f - f_0, y)$can be written as

$$C'(x,y) = \tfrac{1}{2}b(x,y)e^{i[\phi(x,y)+2\pi f_0 x]} \tag{88}$$

Using identical transformation Eq.87 becomes

$$C'(x,y) = \tfrac{1}{2}b(x,y)cos[\phi(x,y) + 2\pi f_0 x] + isin[\phi(x,y) + 2\pi f_0 x] \tag{89}$$

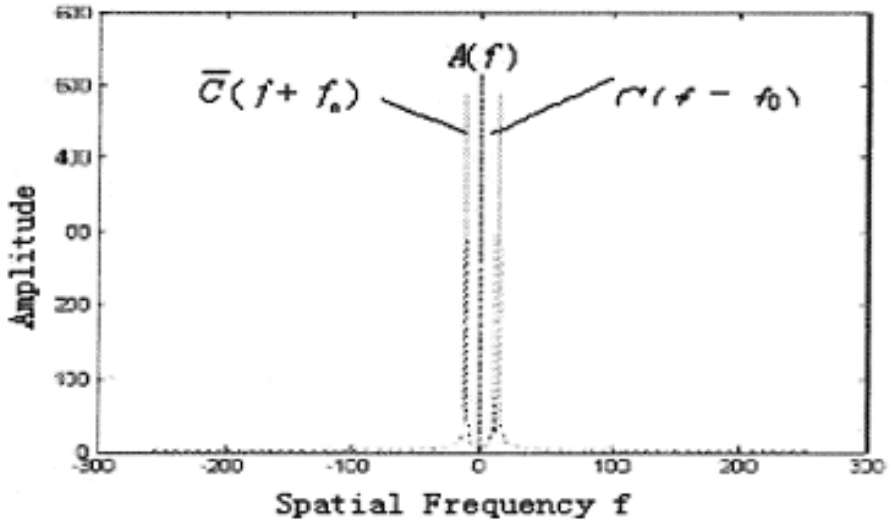

Fig17: Spatial frequency distribution of moiré fringes [15, 30].

Thus the phase factor $\phi(x,y)$ can be extracted from Eq.89

$$\phi(x,y) = arctan\frac{Im(c')}{Re(c')} - 2\pi f_0 x \tag{90}$$

Where $Im(c')$ and $Re(c')$imaginary and real component of complex c'respectively. Because of periodic property of intensity function for moiré fringes, only main phase value can be obtained from moiré fringe pattern by Fourier transform [30, 33].

2.3.5. Diffusion coefficient and Moiré fringe shift

The Moiré Defelectometery experimental set-up is used to measure the diffusion coefficient of transparent solution. The deflected laser beam due to changes in refractive index in the diffusion cell yields the shifted self-image on gratings and resultant Moiré fringes show a deviation [21, 33]. For an isothermal mixture, without generation and recombination, the physical problem associated with the experiment described above can be formulated mathematically. A diffusion column of constant cross-section, extended in the x-direction, and the concentration varying with the position coordinate x only. Thus, the diffusion process can be formulated in terms of one-dimensional problem. The free

diffusion process is governed by Fick's second law, and for one dimensional diffusion along x-axis it is given by:

$$\frac{\partial \vec{c}(x,t)}{\partial t} = D\,\frac{\partial^2 \vec{c}(x,t)}{\partial x^2} \tag{91}$$

Where: - $\vec{c}(x,t)$ is the concentration at position x and time t, D is the diffusion coefficient, assumed to be independent of concentration, and x is the direction of diffusion. If there is the net external force, F (e.g. gravitational force), acting in the x-direction up on the dissolved molecules and if μ be the mobility of the molecules under consideration (i.e. the steady velocity, acquired under the action of unit force) the steady velocity of these molecules would be $\mu.F$ and the resulting flux of matter would be $\mu.\vec{c}F(x,t)$
Consequently the rate of concentration changes would then become:

$$\frac{\partial \vec{c}}{\partial t} = D\,\frac{\partial^2 \vec{c}(x,t)}{\partial x^2} - \mu F\,\frac{\partial \vec{c}(x,t)}{\partial t} \tag{92}$$

It is even possible to reduce the problem of Eq.92 to that of ordinary diffusion Eq.91 by the means of following transformation

$$\vec{c}(x,t) = \vec{c}^{*}(x,t)e^{[\frac{\mu.F}{2D} - \frac{\mu^2 F^2 t}{4D}]} \tag{93}$$

Where $\vec{c}^{*}$ is the function that satisfies Eq.91 If the steady velocity of the dissolved molecules (μF) is very slow the current due to the external forces can be neglected and Eq.92 reduce to Eq.91.The solution of Eq.91, for two binary liquid mixtures initially (t =0) separated at (x =0) with concentration $\vec{c}_0$ and $\vec{c}_1$ is an error function given by

$$\vec{c}(x,t) = \frac{\vec{c}_0 - \vec{c}_1}{2} + \frac{\vec{c}_0 - \vec{c}_1}{2}\; erf[\frac{x}{2\sqrt{Dt}}] \tag{94}$$

Where the error function is defined as

$$erf(x) = \frac{2}{\sqrt{\pi}} \int_0^x e^{-t^2} dt \tag{95}$$

On the other hand, if we consider the solution of Eq.91 in Eq.95, x is replaced by $x - \mu gt$. In this case the influence of gravity causes a change in the central diffusion location, that is another layer as the second center of diffusion will formed [33,36]. In a transparent mixture, a change in the concentration produces a change of refractive index, which for the small concentration gradient can be considered a linear function between refractive index and concentration.

The refractive index gradient is given by

$$\frac{\partial n(x,t)}{\partial x} = \frac{n_0 - n_1}{2\sqrt{\pi} Dt} e^{[-\frac{x^2}{4Dt}]} \tag{96}$$

Where: - $n(x,t)$ is the local index at time t in the diffusion cell, n_0 the refractive index of high concentration solution, and n_1 is of the low concentration solution. If the refractive index changes the rays contributing to the formation of the moiré fringes pattern will be deflected locally according to refractive index distribution, accordingly the Moiré fringes will also change. The incident parallel laser beam passing through the diffusion cell, bends by angle $\varphi(x,t)$ depending on the distribution of the refractive index on the cell. Because the refractive index (concentration) depends on position (x) and time (t), accordingly, the deflection angle also would be position and time dependent. Due to the deflection of the collimated beam, imaging on the defelectometry system, the Fourier image of the first grating shifts on the second grating [15].For small bending of light rays, the amount of Fourier image shift would be $\varphi(x,t)\, Z_t$. The displacement of the Fourier image of the first grating on the second one, the Moiré fringe to shift with respect to the original locations. The amount of fringe shift $\Delta\xi(x,t)$ is given by

$$\Delta\xi(x,t) = \frac{Z(t)}{\theta} \varphi(x,t) \tag{97}$$

Where θ a small tilt angle between the intersection of the grating lines and Z_t is the t[th] Talbot distance between gratings. The desired information from diffusion process is contained in $\varphi(x,t)$.On the other hand, the relation between the integrated deflection angle and the refractive index $n(x,t)$ is

$$\Delta\varphi(x,t) = \frac{1}{n_a}\int_0^L [\frac{\partial n(x,y,z,t)}{\partial x}]_{y=cons.} dz \tag{98}$$

Where $n_a$is the ambient refractive index along the x-axis diffusion, the direction and L represents the thickness of diffusion cell measured along the propagation axis (z-axis). The diffusion process is assumed to occur only along the x -direction, so the index of refraction along the z -direction remain constant and the Eq.98 becomes

$$\varphi(x,t) = \frac{d}{n_a}\frac{\partial n(x,t)}{\partial x} \tag{99}$$

Taking into account Eq.97 and Eq.98 can be written as

$$\Delta\xi(x\,,t) = \frac{Z_t d}{n_a\theta}\frac{\partial n(x,t)}{\partial x} \tag{100}$$

Eq.100, Shows the Moiré Fringe deformation is proportional to the refractive index gradient introduced by the diffusion process [17, 33]. By replacing Eq.98 and Eq.100 the corresponding local shift of Moiré Fringes results

$$\Delta\xi(x\,,t) = \frac{Z_t d}{n_a\theta}\frac{n_0 - n_1}{2\sqrt{\pi}Dt}\, e^{[\frac{-x^2}{4Dt}]} \tag{101}$$

Where for simplicity, Δ_0 defined as

$$\Delta_0 = \frac{Z_t d(n_0 - n_1)}{n_a 2\theta\sqrt{\pi}Dt} \tag{102}$$

$$\Delta\xi(x\,,t) = \frac{\Delta_0 Z_t d}{\sqrt{t}} e^{[\frac{-x^2}{4Dt}]} \tag{103}$$

The diffusion coefficient can be obtained from a single Moiré pattern recorded at time instant t_0. For two distance x_1 and x_2, then $(x_2 > x_1)$ along the diffusion cell, the local shift of Moiré fringes would be [33]

$$\Delta_1 = \frac{Z_t L}{\theta} \frac{n_0 - n_1}{2n_a\sqrt{\pi D t_0}} e^{\left[\frac{-{x_1}^2}{4Dt}\right]} \tag{104}$$

$$\Delta_2 = \frac{Z_t L}{\theta} \frac{n_0 - n_1}{2n_a\sqrt{\pi D t_0}} e^{\left[\frac{-{x_2}^2}{4Dt}\right]} \tag{105}$$

The ratio of two local shift is

$$\eta = \frac{\Delta_2}{\Delta_1} = e^{\left[\frac{-{x_1}^2 - {x_2}^2}{4Dt}\right]} \tag{106}$$

Then the diffusion coefficient can be defined as

$$D = \frac{{x_2}^2 - {x_1}^2}{4t_0 \ln\eta} \tag{107}$$

CHAPTER THREE

Experimental Technique

3.1. Materials used

In carrying out the experiment the following apparatuses were used:-

The 5mW **He-Ne** laser ($\lambda = 632.8$nm) to produce the beam, The diffusion cell of rectangular cross section, Syringes to fill the solution and distilled water into the diffusion cell, plastic bottles to keep different concentration of Ethanol, two Ranchi Gratings each (100 lines/mm) to produce Moiré patterns, the Mercury Thermometer to measure the temperature of the room, expanding and collimating lenses (*f=10cm* each) to magnify the fringes, screen to observe the fringe patterns, CCD(Digital camera with 20.1Mega pixel) to take pictures from the Opal screen, A data cable to connect the digital camera with the computer. Different concentration of ethanol prepared by volume-volume ratio. (eg. To prepare 5% of ethanol solution, from the total 30ml (100%) 1.5ml of ethanol was mixed with 28.5ml of pure water.)

Fig 18:- Different concentration of ethanol and the diffusion cell (cuvette)

3.2. Experimental set-up

The Moiré defelectometry experimental set-up used to measure the diffusion coefficient of different Ethanol solution in pure water at room temperature (23 ± 2^0C). A 5-mW He–Ne laser beam ($\lambda = 632.8$nm) were expanded and collimated. Two similar Rhonchi gratings $\mathbf{G}_1$ and $\mathbf{G}_2$ of 100 lines/mm (with pitch of 0.04mm) were used to construct the Moiré fringe patterns. The distance between planes of $\mathbf{G_1}$ and $\mathbf{G_2}$ was fixed and it is known as one of Talbot distances for the gratings used. Then the Moiré fringes were formed for a fixed Talbot distance. The diffusion cell which is, 15mm thick, 90mm high and 20mm wide the longer dimension gives the direction of diffusion placed in front of grating. The distance separating the inside surfaces is equal to 18mm.

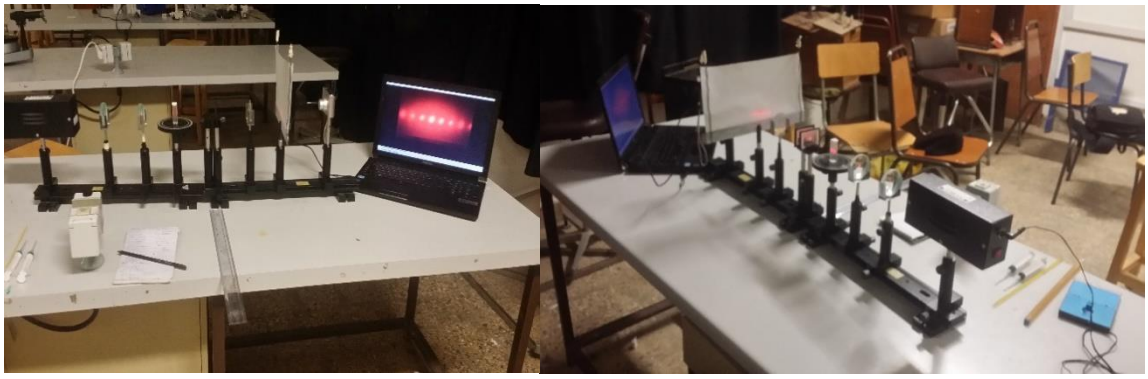

Fig 19: - Experimental set up viewing from near digital camera and near **He-Ne** laser.

3.3. Experimental procedures

The cell was first half-filled with pure water (higher concentration of equal volume) from below using a syringe. After allowing for residual motions to dissipate, the Ethanol solution was slowly injected on the upper part of the diffusion cell; this process takes about 10 seconds. Time was measured from the moment injection was stopped. Then the He-Ne laser is released near the interface on the diffusion cell and the fringes produced by two gratings are magnified using microscopic lens placed at the back of second grating. Finally

the Grating patterns, during the evolution of diffusion phenomena, are captured from the opal screen at different time interval by digital camera and are stored in the computer.

CHAPTER FOUR

Results, Analysis and Discussion

4.1. Determination of diffusion coefficient of ethanol solution in different concentration

The diffusion coefficient of a solute in solvent depend on temperature, concentration, size of particle, position and the time taken for diffusion. The concentration of solution in this experiment is also the function of position and time taken keeping the temperature constant. The following figures and data analysis for the diffusion coefficients were made for various concentration of Ethanol solution at room temperature.

4.1.1. Results obtained for 5 % of ethanol solution

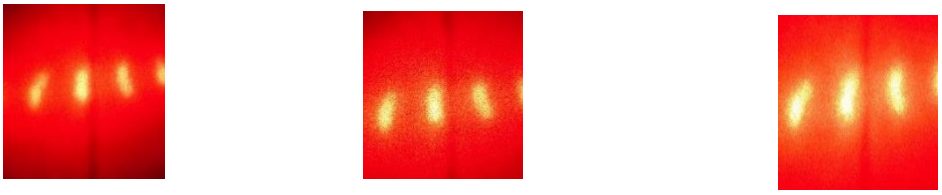

$t_0 = 0,$ $t_1 = 90\text{min}$ $t_2 = 2hr$

Fig 4.1: Fringe shift in 5 % of ethanol solution

Table 1. Fringe shifts in 5% of ethanol solution after $t_0 = 0, t_1 = 90\text{min. and } t_2 = 2hr$

Time (hrs.)			Shift(cm)			Local shift(cm)		Ratio of local shift	Diffusion coefficient
t_0	t_1	t_2	x_0	x_1	x_2	Δ_1	Δ_2	η	D(x10^{-5}cm^2/s)
0	1 ½	2	0.655	0.68	0.785	0.025	0.105	0.238	0.616

4.1.2. Results obtained for 10 % of ethanol solution

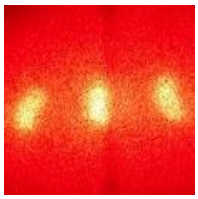

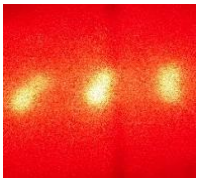

$t_0 = 0,$ $t_1 = 2\text{hr}.$ $t_2 = 2\frac{1}{2}\text{hr}$

Fig 4.2:- Fringe shift in 10 % of ethanol solution

Table2. Fringe shifts in 10 % of ethanol solution after $t_0 = 0, t_1 = 2\text{hr}.\text{and}\ t_2 = 2\frac{1}{2}\text{hr}$

Time (hrs.)			Shift(cm)			Local shift(cm)		Ratio of local shift	Diffusion coefficient
t_o	t_1	t_2	x_0	x_1	x_2	Δ_1	Δ_2	η	D(x10^{-5}cm^2/s)
0	2	2 ½	0.66	0.75	0.846	0.09	0.096	0.937	0.715

4.1.3. Results obtained for 15 % of ethanol solution



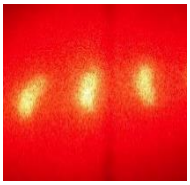

$t_0 = 0,$ $t_1 = 2\frac{1}{2}\text{hr}$ $t_2 = 3\text{hr}$

Fig 4.3: Fringe shift in 15% of ethanol solution

Table 3.Fringe shifts in 15 % of ethanol solution after $t_0 = 0, t_1 = 2\frac{1}{2}\text{hr}\ \text{and}\ t_2 =$ 3hr

Time (hrs.)			Shift(cm)			Local shift		Ratio of local shift	Diffusion Coefficient
t_o	t_1	t_2	x_0	x_1	x_2	Δ_1	Δ_2	η	D(x10^{-5}cm^2/s)
0	2 ½	3	0.65	0.74	0.87	0.09	0.13	0.692	0.76

4.1.4. Results obtained for 20 % of ethanol solution

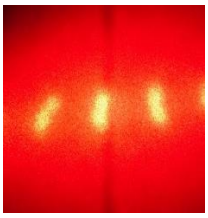

$t_0 = 0,$

$t_1 = 3\text{hr. and}$

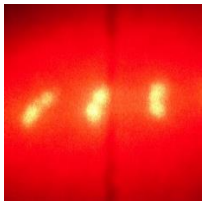

$t_2 = 3\frac{1}{2}\text{hr}$

Fig 4.4: Fringe shift in 20% of ethanol solution

Table 4. Fringe shifts in 20 % of ethanol solution after $t_0 = 0, t_1 = 3\text{hr. and } t_2 = 3\frac{1}{2}\text{hr},$

Time (hrs.)			Shift(cm)			Local shift(cm)		Ratio of local shift	Diffusion coefficient
t_o	t_1	t_2	x_0	x_1	x_2	Δ_1	Δ_2	η	D(x10^{-5}cm^2/s)
0	3	3 ½	0.657	0.805	0.89	0.148	0.085	1.74	0.792

4.1.5. Results obtained for 25 % for ethanol solution

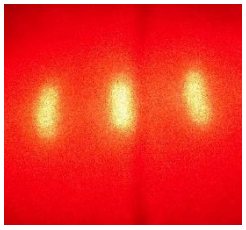

$t_0 = 0,$

$t_1 = 3\frac{1}{2}\text{hr.}$

$t_2 = 4\text{hr},$

Fig 4.5: Fringe shift in 25% of ethanol solution

Table.5.Fringe shifts in 25% of ethanol solution after $t_0 = 0, t_1 = 3\frac{1}{2}\text{hr.and } t_2 = 4\text{hr},$

Time (hrs.)			Shift(cm)			Local shift		Ratio of local shift	Diffusion coefficient
t_o	t_1	t_2	x_0	x_1	x_2	Δ_1	Δ_2	η	D(x10^{-5}cm^2/s)
0	3 ½	4	0.636	0.861	0.912	0.2	0.251	0.8	0.832

4.1.6. Results obtained for 30% of ethanol solution

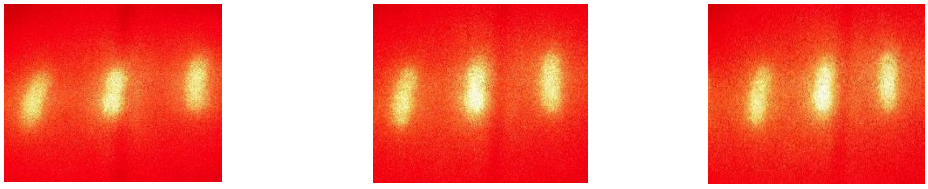

$t_0 = 0,$ $t_1 = 4hr$ $t_2 = 5hr,$

Fig 4.6: Fringe shift in 30% of ethanol solution

Table 6. Fringe shifts in 30% of ethanol solution after $t_0 = 0, t_1 = 4hr.$ and $t_2 = 5hr,$

Time (hrs.)			Shift(cm)			Local shift(cm)		Ratio of local shift	Diffusion coefficient
t_o	t_1	t_2	x_0	x_1	x_2	Δ_1	Δ_2	η	$D(x10^{-5}cm^2/s)$
0	4	5	0.65	0.867	0.92	0.217	0.053	4.1	0.846

4.1.7. Results obtained for 35 % of ethanol solution

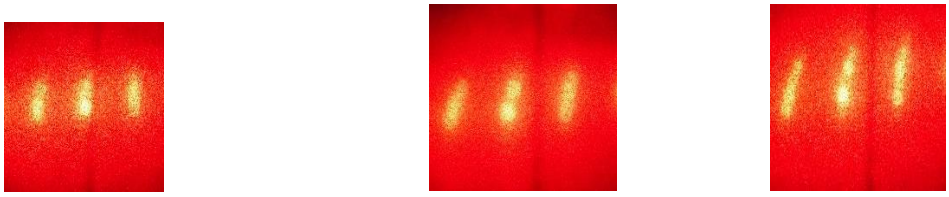

$t_0 = 0,$ $t_1 = 5hr.$ $t_2 = 5\frac{1}{2}hr,$

Fig 4.7: Fringe shift in 35 % of ethanol solution

Table 7. Fringe shifts in 35 % of ethanol solution after $t_0 = 0, t_1 = 5hr.$ and $t_2 = 5\frac{1}{2}hr,$

Time (hrs.)			Shift(cm)			Local shift(cm)		Ratio of local shift	Diffusion coefficient
t_o	t_1	t_2	x_0	x_1	x_2	Δ_1	Δ_2	η	$D(x10^{-5}cm^2/s)$
0	5	5 ½	0.654	0.882	0.94	0.23	0.058	3.9	0.884

4.1.8. Results obtained for 40 % of ethanol solution

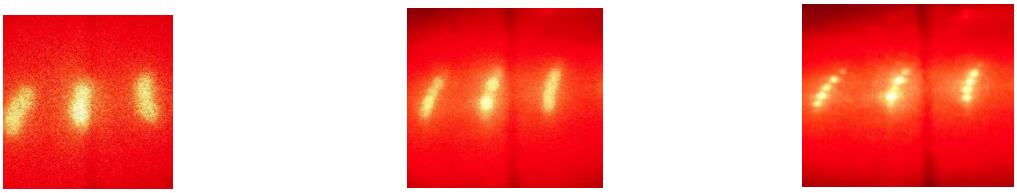

$t_0 = 0$, $t_1 = 6\text{hr}$ $t_2 = 6\frac{1}{2}\text{hr}.$

Fig 4.8: Fringe shift in 40% of ethanol solution

Table 8. Fringe shifts in 40% of ethanol solution after $t_0 = 0, t_1 = 6\text{hr}$ and $t_2 = 6\frac{1}{2}\text{hr}$.

Time (hrs.)			Shift(cm)			Local shift		Ratio of local shift	Diffusion Coefficient
t_o	t_1	t_2	x_0	x_1	x_2	Δ_1	Δ_2	η	$D(x10^{-5}cm^2/s)$
0	6	6 ½	0.65	0.891	0.98	0.24	0.089	2.71	0.96

4.1.9. Results obtained for 50% of ethanol solution

$t_0 = 0$, $t_1 = 8\text{hr}$ and $t_2 = 9\text{hr}$

Fig 4.9: Fringe shift in 50% of ethanol solution

Table 9. Fringe shifts in 50% of ethanol solution after $t_0 = 0, t_1 = 8\text{hr}$ and $t_2 = 9\text{hr}$,

Time (hrs.)			Shift(cm)			Local shift		Ratio of local shift	Diffusion Coefficient
t_o	t_1	t_2	x_0	x_1	x_2	Δ_1	Δ_2	η	$D(x10^{-5}cm^2/s)$
0	8	9	0.66	0.899	1	0.24	0.10	2.36	1.0008

4.2. Discussion

Moiré defelectometery provides data about changes of concentration/refractive index between two different solutions. The Moiré pattern shown in the beginning of the experiment is when the laser beam scans a uniform area. As the heavier solution in the lower part of the diffusion cell pushes the lighter solution to the top of the cell, the moiré fringes, due to both solutions, would be seen simultaneously. The refractive indices at various planes along the diffusion cell are different and the liquid passing through the cell will have different optical paths. In a transparent mixture, change in concentration for a multi-component liquid mixture, results in the change in index of refraction. A parallel laser beam passing through such a medium of varying index of refraction, is locally deflected even if it passes perpendicularly to the gradient of index of refraction in the diffusion direction. The deflection angle is direct mapping of the refractive index gradient of the medium. In the Moiré defelectometry technique, the monitored area is restricted by the laser beam and grating size. For the wide/expand laser beam and larger grating size it is possible to monitor large areas of diffusion cell.

As we can see from table (1-9) the diffusion coefficient obtained for some concentration of Ethanol in pure water at room temperature using Moiré defelectometry technique is in good agreement with the diffusion coefficient obtained by other researchers using other techniques like :

In 30 percent ethanol solution the value of the diffusion coefficient found was D = (0.846$\pm$ 0.02) X10^{-9}m^2/s. This value is comparable with the one found by empirical correlation, Cussler, E. L. [18] which was D = 0.84 X10^{-9}m^2/s

In 40 percent ethanol solution the value of the diffusion coefficient is found to be D = 0.96 x10^{-9}m^2/s. The obtained value is also comparable with that is found by theoretical correlation, Wilke. C.R. et al. [19] which was: D = 0.96 X10^{-9}m^2/s.

In 50 percent ethanol solution the value of diffusion coefficient obtained was D = (0.99 $\pm$ 0.02) x10^{-9}m^2/s. This value is comparable to that one found by Wilke.C.R. Empirical finding method which is equal to D = 1 x10^{-9}m^2/s.

To some up, the average value of the diffusion coefficient (D) is found to be (0.822± 0.02) X $10^{-9}m^2/s$.

4.3. Diffusion Vs concentration graph

In transparent solution change in the concentration produces the change of refractive indices, that results in the deflection of angle. Due to the deflection of collimated beam on the defelectometery system the displacement of image of the first grating cause fringe shift from original direction.

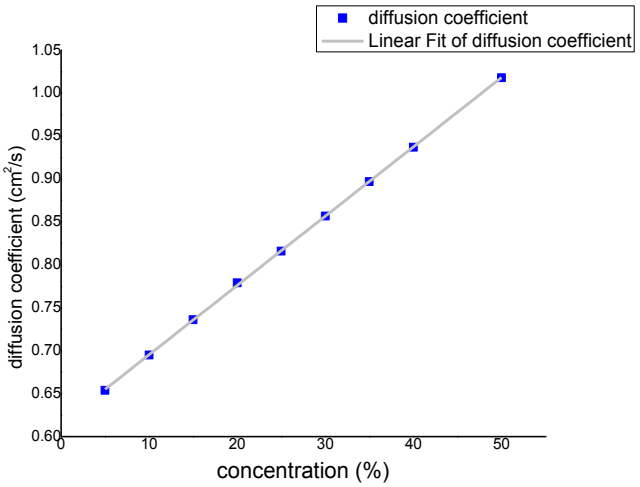

Fig 4.3.1 Diffusion Vs concentration graph

Table 10: The result of slops and intercept for Diffusion Vs concentration graph

Equation	y = a + b*x		
Adj. R-Square	0.9999		
		Value	Standard Error
diffusion coefficient	Intercept	0.61482	8.47066E-4
diffusion coefficient	Slope	0.00807	2.91495E-5

From the graph we can see that, in transparent solutions the diffusion coefficient and small concentration gradient can be a linear function between refractive index and concentration.

CHAPTER FIVE

Conclusion and Recommendation

5.1. Conclusion

Moiré defelectometery is a power tool for determining diffusion coefficient of transparent liquid solution and it includes direct mapping of ray deflection due to the change of refractive index of diffusion medium. This leads to local perturbation of a collimated laser incident beam which is mapped by Moiré firings patterns. From the experiment conducted (table 1-9), the average value of the diffusion coefficient (D) obtained was (0.822 ± 0.02) $x10^{-9} m^2/s$, and it is in good agreement with the reported values in literatures using other methods [18, 19]. The result shows that ray deflection increase linearly with the increase in concentration and increase the index of refraction of the solution. As we have seen for different concentration of ethanol the diffusion coefficient is nearly similar but the rate of diffusion varies with concentration. Also, the Moiré fringes shift due to the refractive index distribution inside the diffusion cell describes, the relationship between the change in the moiré fringes and the deflection angle of the laser beam that passes through the diffusion cell.

5.2. Recommendation

The research was carried out on different concentration of ethanol in pure water at the same temperature. Ethanol is used for different purposes. It is widely available and easy to use. It is also renewable source that can be reused. Ethanol is used as alternative liquid fuel for Automobile because when it is mixed with petrol in some proportion it undergoes complete combustion. This helps for the reduction of greenhouse gas emission (emits low CO and CO_2 to air). And also used as petrol extender and therefore reduce consumption of petrol.

Therefore, we recommended that it is better to do on the mentioned use of ethanol especially in Ethiopia.

BIBLIOGRAPHY

[1] Brendo G. Hewitt (2005): Alcohol Microsoft R Encarta R Encyclopedia: NIAAA: 'Harmful of Alcohol use'.

[2] Son, C.H., and Topyan, K. (2011): The Effect of Alcoholic Beverage Excise Tax on Alcohol-Attributable Injury Mortalities. *Euro. J. Health Eco. 12: 103–113*

[3] Arrizon, J. Calderón, C. and Sandoval, G. (2006): Effect of Different Fermentation Conditions on the Kinetic Parameters and Production of Volatile Compounds during the Elaboration of a Prickly Pear Distilled Beverage. *J. Ind. Mic.bio. Biotech. 33: 921–928.*

[4] Sahle S and Gashe BA (1991): The microbiology of tella fermentation. SINET: Ethiop. J. Sci.14:81-92.

[5] Bahiru B, Mehan T and Ashenafi M (2001): Chemical and nutritional properties of tej, an Indigenous Ethiopian honey wine: variations within and between production units. *J Food Technol Africa. 6:104-8.*

[6] Yohannes T, Melak F and Siraj K (2013): Preparation and physicochemical analysis of some Ethiopian traditional alcoholic beverages. *African J Food Sci.7:399-403.*

[7] Abegaz K. (2013): Isolation, characterization and identification of lactic acid bacteria involved in traditional fermentation of borde, an Ethiopian cereal beverage. *African J Food Sci Res.1:24-32.*

[8] Bacha K, Mehari T and Ashenafi M (1999): Microbiology of the fermentation of shamita, a traditional Ethiopian fermented beverage. SINET: Ethiop J Sci.22:113 –26.

[9] Alemu F, Amha-Selassie T, Kelbessa U, Elias S (1991): Methanol, fuel oil and ethanol Contents of some Ethiopian traditional alcoholic beverages. SINET: Ethiop. J. Sci. 14:19-27.

[10] Ghebrekidan H (1992): The effect of different chemical and physical agents on the viability of Cysticercus bovis: a preliminary report. Ethiop. Med. J. 30:23-31.

[11] World Health Organization (WHO) (2004): Global Status Report on alcohol.

[12] Brust, J. C. M. (2010). "Ethanol and Cognition: Indirect Effects, Neurotoxicity and Neuroprotection: A Review". *Int. J. Env. Res. Pub. Health*. 7 (4):

[13] National Institute of Health. (2000) National Institute on Alcohol Abuse and Alcoholism. p. 134. Retrieved 21 October 2014.

[14] Arun Anand, K.Vanic Chhaniwal and CS Narayana Murthy, (2002,) Diffusivity Study of Transparent Liquid Solution by Imaging Beam Deflection.

[15] Crank E.J. (1975). The Mathematics of Diffusion. Oxford University Press, Oxford.

[16] Schirripa Spagnolo, Ambrosini, and Paoletti. (2004). Liquid Diffusion coefficients by Digital Moiré. Optical Engineering, Vol. 43 No. 4.

[17] Kazem Jamshidi-Ghaleh.K, Mohammad Taghi Tavasoly.M and Nastaran Mansour. (2004) 1993–1997, Diffusion Coefficient Measurements of Transparent Liquid Solutions Using Moiré Defelectometery. J. Phys. D: Appl. Phys. 37.

[18] Cussler, E. L. (1997). Diffusion: Mass Transfer in Fluid Systems (2nd Ed.). New York: Cambridge University Press.

[19] Wilke, C. R. (1949), Estimation of Liquid Diffusion Coefficients. Chem.Eng. Prog.45, 218

[20] John Wiley and Sons, Inc. (1992), Moiré and Fringe Projection Techniques Optical Shape Testing, second Edition, and Edited by Denial Malacra.

[21] Weiss, G. (1994). Aspects and Applications of the Random Walk. North-Holland.

[22] Kafri O. and Glatt I. (1986). Moiré Defelectometery: A Ray Deflection Testing Opt.Eng.24.

[23] Jost.W. (1970), Diffusion in Solids, Liquids, and Gas. New York: Academic.

[24] N. Rashidnia, R. Balasubramaniam, J. Kuang, P. Petitjeans and T.Maxworthy. (2001), Measurement of the Diffusion Coefficient of Miscible Fluids Using Both Interferometry and Wiener's Method-*Int. J. Ther. Phys*, Vol.22, No. 2.

[25] Patroski K (1989), the self-imaging phenomenon and its applications Progress in Optics vol. 27, Ed E Wolf (Amsterdam: North-Holland) pp. 1– 108.

[26] N.J Giordon, H. (1997), Prentice Computational Physics.

[27] Mayinger F(Ed) (1994), Optical Measurements (Berlin: Springer).

[28] Moor, D.T. and B.E.Truax, (1979), Phase-Locked Moiré Fringe Analysis for Automated Countering of Diffuse Surfaces Appl.Opt.18 (1), 91-96

[29] Kung H, L.Bhatnager A and Muiller DAB. (2001), Opt.Lett 26 1645.

[30] MacGovern, A.J, (1972), Projected Fringes and Holography, Appl.Opt11 (12), 2972-74.

[31] Guild J. (1956), the Interference Systems of Crossed Diffraction Gratings, Cloreodon Press, Oxford.

[32] Steven L.Jacques, Scott A.Prahl, (1998), Fick's Laws of Diffusion; ECE532 Bio-Medical Optics.

[33] Krasinki M.J (1996), Evolution of Diffusion fildes around KDP Crystal growing in gel crystal. Res.Technol 34.

[34] Mathur B.K. (1966). Principle of Optics, Academic Press Ince.New York.

[35] L.Mertz, (1983), Real-Time Fringe Pattern Analysis Appl Opt Vol 22 No 10 P 1535.

[36] Howard .M.Smith (1969), Principle of Holography, Printed in the United States of America.